



Cite this: DOI: 10.1039/d4ma00502c

# Sulfur quantum dots for fluorescence sensing in biological and pharmaceutical samples: a review

Kawan F. Kayani,<sup>id</sup>\*<sup>ab</sup> Sewara J. Mohammed,<sup>id</sup><sup>cd</sup> Nian N. Mohammad,<sup>ae</sup>  
Ahmed M. Abdullah,<sup>a</sup> Diary I. Tofiq,<sup>a</sup> Muhammad S. Mustafa,<sup>a</sup> Dler M. S. Shwan<sup>a</sup>  
and Shujahadeen B. Aziz<sup>df</sup>

The creation of uncomplicated and efficient sensors for achieving specific analyte detection can provide valuable information for on-site analysis. Sulfur quantum dots (SQDs), an innovative category of fluorescent nanomaterials, are currently under study and applied in diverse fields, with a primary focus on fluorescence (FL) sensing. These SQDs offer several advantages, such as a straightforward synthesis method, distinct composition, extremely small size, customizable fluorescence, and minimal toxicity. This review focuses on fluorescent sensors designed based on SQDs, emphasizing the detection of specific targets in human biological samples, as well as in pharmaceutical samples. Finally, this paper addresses the future development and critical challenges associated with the detection of many targets based on SQDs as probes in different fields.

Received 14th May 2024,  
Accepted 8th July 2024

DOI: 10.1039/d4ma00502c

rsc.li/materials-advances

## 1. Introduction

In recent decades, considerable research has focused on the photophysical properties and applications of various small particles, including quantum dots (QDs)<sup>1–5</sup> and nanoclusters (NCs).<sup>6–8</sup> Terminologies like nanomaterials, nanorods, and nanoplates have also been used to describe specific nanoscale materials. Notably, size-dependent photoluminescence (PL) resulting from quantum confinement effects is a widely explored phenomenon in the fields of chemical and biological research.<sup>9</sup> This burgeoning nanoscience has made its way into educational settings across all levels.<sup>10,11</sup> QDs have attracted much attention for a variety of promising applications<sup>12–14</sup> in catalysis,<sup>15,16</sup> analysis,<sup>4,17–21</sup> energy conversion/storage,<sup>22</sup> bio-imaging and biomedicine,<sup>23,24</sup> and drug delivery,<sup>25</sup> as well as sensing applications in food analysis.<sup>26</sup>

Zero-dimensional nanomaterials (0D NMs) have garnered considerable interest in sensing applications, including metal

NCs<sup>27</sup> and carbon dots (CDs).<sup>28</sup> However, metal NCs, due to their heavy metal composition, pose significant health and environmental concerns<sup>29</sup> and exhibit low stability.<sup>30</sup> Recently, SQDs, a new type of non-metallic quantum dot from the nanosulfur family, have emerged as promising fluorescent materials. SQDs feature a polymeric sulfur core and exhibit impressive photophysical properties,<sup>31</sup> along with inherent characteristics such as non-toxicity, hydrophilicity, and anti-bacterial properties.<sup>32</sup> Governed by lone pair electrons, sulfur atoms have a notable affinity for analytes.<sup>33</sup> Therefore, the successful synthesis and appealing attributes of SQDs present new opportunities for chemical sensing compared to other QDs.

Elemental sulfur, among the most abundant natural resources, boasts a history of utilization spanning thousands of years. In the 19th century, sulfur deposits in volcanic rocks dominated its extraction. Presently, global elemental sulfur primarily arises from desulfurization in natural gas and crude oil refining, yielding over 70 million tons annually.<sup>32,34</sup> Beyond sulfuric acid production, it finds applications in medicine, agriculture, and the rubber industry. Despite meeting elemental sulfur demands, a substantial excess persists, resulting in significant waste and storage risks due to its inflammable and explosive nature. Urgent exploration of effective approaches for the value-added utilization of elemental sulfur is essential. Earth-abundant sulfur, ranked 14th in elements found in the Earth's crust, plays a pivotal role in various fields,<sup>35</sup> including sulfuric acid production, lithium–sulfur batteries, and modifications in polymeric and organic materials. Unlike other chemical commodities, sulfur is involuntarily produced from natural gas processing and petroleum refineries, producing

<sup>a</sup> Department of Chemistry, College of Science, University of Sulaimani, Qliasan St, 46002, Sulaimani City, Kurdistan Region, Iraq.

E-mail: kawan.nasraddin@univsul.edu.iq

<sup>b</sup> Department of Chemistry, College of Science, Charmo University, Peshawa Street, Chamchamal, Sulaimani City, 46023, Iraq

<sup>c</sup> Anesthesia Department, College of Health Sciences, Cihan University Sulaimaniya, Sulaimaniya 46001, Kurdistan Region, Iraq

<sup>d</sup> Research and Development Center, University of Sulaimani, Qlyasan Street, Kurdistan Regional Government, Sulaymaniyah, 46001, Iraq

<sup>e</sup> Department of Medical Laboratory Science, College of Science, Komar University of Science and Technology, Sulaimani, 46001, Iraq

<sup>f</sup> Department of Physics, College of Science, Charmo University, Chamchamal, Sulaymaniyah, 46023, Iraq



more than 7 million tons of high-quality sulfur each year. The fascinating attributes of this material, including its notable capabilities for high alkaline metal storage, molar refraction, infrared transparency, and pesticidal properties, underscore its significance in diverse applications.<sup>36</sup>

Sulfur nanoparticles (SNPs)<sup>11</sup> are widely utilized, yet their practical use is limited due to challenges such as large particle size, insufficient hydrophilicity, low reactivity, and toxicity. To address their toxicity, the inherent attributes of SQDs, such as non-toxicity, hydrophilicity, and ease of modification, have bolstered their potential for sensing applications.<sup>37,38</sup>

In recent times, researchers have turned their focus to a fresh entrant in the realm of pure elemental quantum dots (SQDs). This exploration has brought to light their improved photocatalytic and FL properties. Various approaches, including mechanical methods like ultrasonication<sup>39</sup> and microwave treatment,<sup>40</sup> as well as chemical strategies such as pure O<sub>2</sub> oxidation,<sup>41</sup> have been employed to expedite the synthesis of SQDs and enhance their quantum yield. The transition from bulk sulfur to S dots has unveiled unexpectedly delightful optical properties.<sup>42</sup> Consequently, the successful synthesis and enticing features of SQDs pave the way for advancements in chemical sensing,<sup>43</sup> white light-emitting diodes,<sup>44</sup> catalysis,<sup>45</sup> and bioimaging.<sup>46</sup> Governed by lone pair electrons, sulfur atoms consistently demonstrate an affinity toward specific targets, leveraging fluorometric signals from the probe.

The aim of this review is to offer a comprehensive understanding of the current research status of SQDs. After providing a brief introduction to SQDs and their characteristics, we delve into their applications. Our unique contribution lies in introducing their applications for the first time in biological molecules and pharmaceutical drugs, utilizing FL sensing techniques. This opens up new avenues for their practical utilization in biological and pharmaceutical analyses.

## 2. Sulfur quantum dots and synthesis

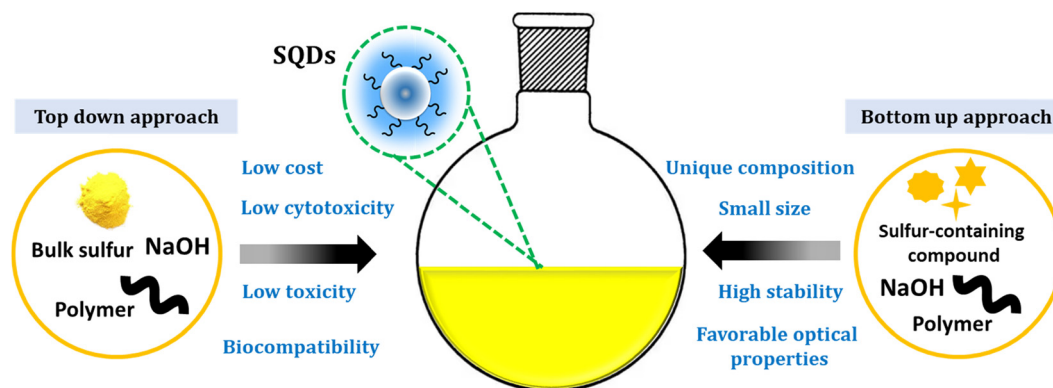
Sulfur quantum dots represent a fascinating and innovative class of nanomaterials that have gained considerable attention

in recent years.<sup>47,48</sup> SQDs arise as an innovative class of luminescent nanomaterials, displaying considerable potential across diverse application domains.<sup>36</sup> Since their initial report in 2014,<sup>37</sup> SQDs have garnered substantial interest as emerging and active metal-free elemental quantum dots. Their unique composition, favorable optical properties, low toxicity, small size, ease of processing, and cost-effectiveness enhance their promising profile.<sup>49,50</sup> Additionally, comprising a polymeric sulfur core embellished with abundant surface functionalities like sulfites and sulfates, SQDs exhibit excellent water dispersibility. The presence of these surface functional groups, combined with polar functional groups from the surface passivation agent, makes them ideal candidates for surface functionalization. Notably, the unique photophysical properties of SQDs make them versatile for a myriad of applications.<sup>31</sup>

Over the last five years, there has been a remarkable surge in interest in sulfur quantum dots, an innovative category of metal-free fluorescent quantum dots. This heightened attention is attributed to their distinct optical, spectroscopic, chemical, and antibacterial properties.<sup>40</sup> Scheme 1 illustrates the properties of SQDs.

Direct synthesis of SQDs from readily available and affordable elemental sulfur has been achieved. A multitude of researchers have attempted to explore the diverse application possibilities of SQDs. Up to now, multiple methods have been developed to produce fluorescent SQDs, and these methods can be categorized into two groups. The initial classification, referred to as the bottom-up approach, involves directly oxidizing or reducing sulfur ions present in compounds containing sulfur, such as metal sulfides and thiosulfates, to produce zero-valent sulfur atoms. For instance, Li and colleagues generated fluorescent SQDs by oxidizing S<sup>2-</sup> ions into zero-valent S atoms through an interfacial reaction involving metal sulfide quantum dots and nitric acid.<sup>51</sup> This approach includes creating fluorescent SQDs by utilizing sodium thiosulfate as the primary material in conjunction with solution chemistry. This overcomes the limitation of the extended reaction times associated with using elemental sulfur directly as the raw material (Fig. 1A).<sup>52</sup>

An alternative synthesis strategy is the top-down approach, wherein fluorescent SQDs are directly synthesized from



Scheme 1 Summary of sulfur quantum dots and their properties.



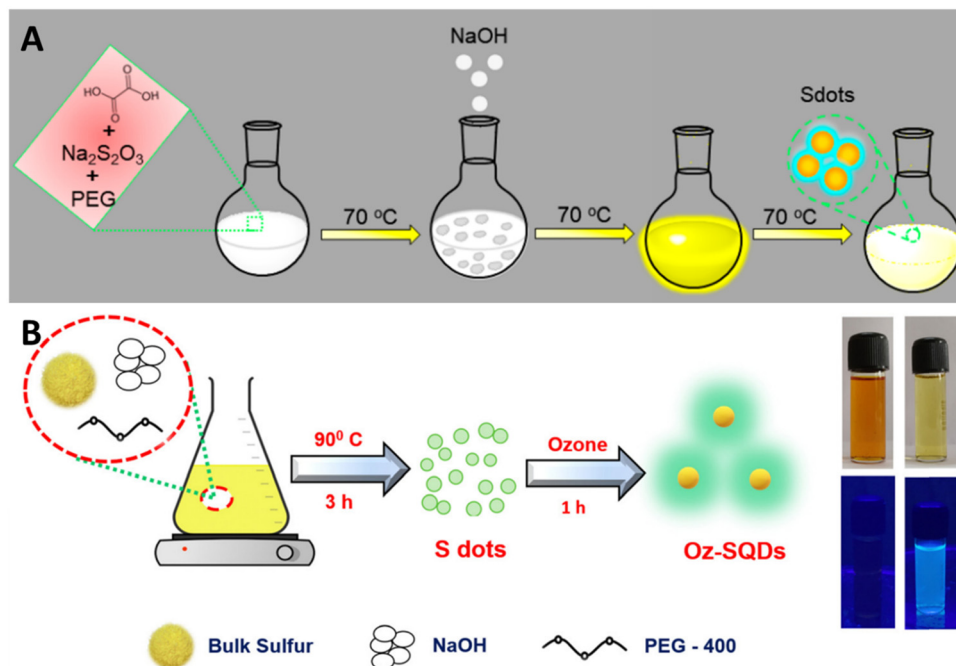


Fig. 1 Diagrammatic representation of SQD synthesis using (A) the bottom-up approach; from ref. 52 with permission, Copyright 2020, American Chemical Society; and (B) top-down method from ref. 53. With permission. Copyright 2023, Royal Society of Chemistry.

elemental sulfur *via* solution chemistry under varying reaction conditions. For example, Biju *et al.*<sup>53</sup> efficiently produced luminescent SQDs utilizing cost-effective and abundant bulk sulfur powder. This process entails dissolving bulk sulfur powder into small particles in an alkaline environment, followed by the oxidation of polysulfide ions to zero-valent sulfur by ozone. The utilization of ozone's robust oxidizing potential has significantly shortened the synthesis time to just 4 hours. The obtained Oz-SQDs exhibit nearly uniform size, customizable emission, colloidal stability, robust thermal stability, and outstanding photostability. Additionally, they achieved a reasonable PL quantum yield of 9.26% (Fig. 1B). This work paves the way for the direct production of cost-effective and readily available fluorescent SQDs from elemental sulfur.

Therefore, the research and development of highly luminescent SDs have long-term significance for practical applications.

### 3. Sensing mechanism

FL sensing represents a rapidly evolving domain in research and technology, encompassing the detection of a wide array of natural and synthetic compounds across various media, including living organisms. Its applications span from overseeing industrial processes to monitoring environmental conditions and diagnosing medical conditions.<sup>54</sup> Among the myriad of detection techniques available, FL methods stand out for their unparalleled sensitivity, precise temporal and spatial resolution, and adaptability, enabling not only remote detection of diverse targets but also the visualization of targets.<sup>29</sup> At the core of sensing lies the transmission of signals generated by

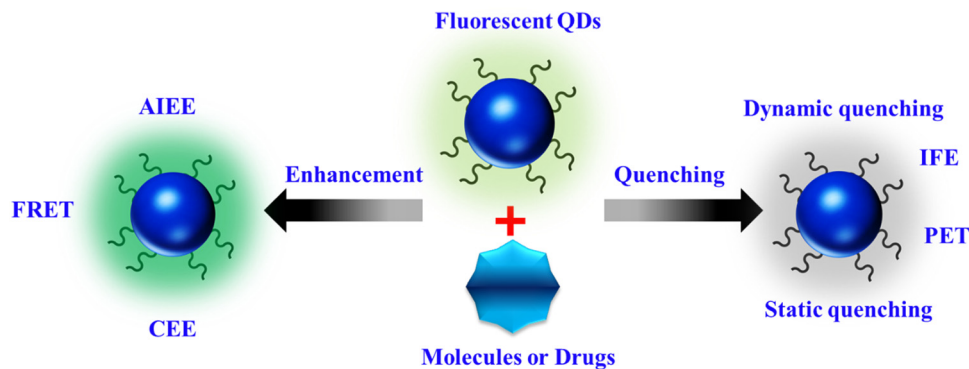
molecular interactions with the target to fluorescent molecules, nanoparticles, and nanocomposites, which are then detected using state-of-the-art electronic and optical devices.

The fluorescent properties of materials are influenced by their synthesis method, shape, and surrounding environment. Alterations in bonds, energy, or electron transport processes lead to the enhancement or reduction of FL quality as a result of interactions between fluorescent materials and external substances. As illustrated in Scheme 2, we categorize the FL-based strategies into “FL quenching” and “FL enhancement” techniques. The subsequent section elaborates on the potential fluorescence mechanisms, along with recent applications.

#### 3.1. FL quenching

Numerous biochemical analyses have been proposed using FL quenching of fluorophores by analytes. The FL intensity can be reduced through various processes with distinct mechanisms, collectively known as quenching. Dynamic quenching, particularly collisional quenching, occurs when excited-state fluorophores are deactivated upon contact with other molecules (quenchers), resulting in a charge or energy transfer. This dynamic quenching leads to a reduction in the excited-state lifetime of the fluorophore with increasing quencher concentration, regardless of the fluorophore absorption spectral profile. Photoinduced electron transfer (PET) is a type of dynamic quenching in which electron transfer from the highest occupied molecular orbital (HOMO) of the analyte to the fluorophore causes FL quenching. In cases involving transition metal ions, electrons may transfer from the fluorophore to the analyte, leading to FL quenching.<sup>55</sup>





Scheme 2 Proposed mechanisms for FL quenching and FL enhancement techniques.

The inner filter effect (IFE) is another FL quenching mechanism that results from the overlap between the absorption spectra of the absorber and the excitation and/or emission spectra of the fluorophore. In this scenario, energy from the excitation source and/or emission of the fluorophore is absorbed by the absorber. Key factors influencing the IFE mechanism include the independence of the excited-state lifetime of the fluorophore on the presence or absence of the absorber, the dependence of quenching efficiency on the excitation and emission wavelength of the fluorophore, and the absence of changes in the absorption spectrum of the fluorophore in the presence of the absorber.<sup>29</sup>

Static quenching occurs when fluorescent materials form non-fluorescent complexes with quenchers. This interaction typically occurs in the ground state; upon light irradiation, the system returns to the ground state without emission. Static quenching is characterized by changes in the absorption spectra of the fluorophore, independence from the excited-state lifetime of the fluorophore, and an increase in FL with increasing temperature.<sup>56</sup>

### 3.2. FL enhancement

Fluorescence enhancement can be attributed to aggregation-induced emission enhancement (AIEE), FL resonance energy transfer (FRET), and the crosslink-enhanced emission effect (CEE).

Aggregation-induced emission enhancement (AIEE) occurs when fluorophores aggregate or crystallize, leading to intensified emission. Normally, in solution, organic compounds with freely rotating groups do not emit light; however, upon crystallization or aggregation, their rotational freedom becomes restricted, resulting in fluorescence.<sup>57</sup> FRET is a nonradiative process of energy transfer based on dipole-dipole interactions between fluorescent molecules. Energy transfer occurs rapidly from a donor molecule to an acceptor molecule within a proximity of 0 to 10 nm without photon emission.<sup>58</sup> CEE involves the amplification of luminescence due to crosslinking. This phenomenon is believed to arise from aggregated or crosslinked polymer structures or sublumino-phore functional groups that emit light. Chemical or physical crosslinking, whether through covalent or non-covalent bonds, can induce crosslinking. Covalent bonds create stable and robust bonding

interactions, imparting rigidity and preventing non-radiative transitions. Non-covalent interactions include supramolecular interactions, complexation with ions, and interactions within confined domains.<sup>59</sup>

## 4. Applications

### 4.1. Biosensing

Biosensing, employing the captivating characteristics of SQDs, is a developing domain where a variety of methods are employed to identify different targets such as ions,<sup>60–62</sup> small molecules,<sup>48,63,64</sup> and temperature sensing.<sup>65</sup> Owing to their high chemical stability, favorable aqueous solubility, straightforward surface functionalization, and inherent antimicrobial attributes, SQDs can enhance detection sensitivity and selectivity.

**4.1.1. Small molecule sensing.** The luminescence properties of SQDs make them a valuable tool for detecting biologically significant small molecules. Ascorbic acid (AA), a vital organic nutrient recognized as vitamin C, has extensive applications in food additives, healthcare supplements, and medications for enhancing human well-being.<sup>66</sup> AA exhibits robust reducibility, consistently serving as a potent antioxidant to mitigate oxidative stress in physiological metabolism, particularly as a substrate for ascorbate peroxidase.<sup>67</sup> Furthermore, AA plays a crucial role in various biosynthetic processes, including collagen formation, metabolism of tyrosine and tryptophan, iron utilization, normal development of bone and dentin cells, and enhancement of immune activity.<sup>68,69</sup> Therefore, it is crucial to monitor the concentration of AA in biological samples for medical diagnosis.

A FL probe based on water-soluble SQDs was created using an uncomplicated, environmentally friendly, and highly efficient one-pot synthesis method, which exhibited a remarkably high quantum yield. This probe was successfully designed for the swift and discernible detection of Ce(IV). Moreover, the system has been proven effective in various Ce(IV)-related biological assays, including the analysis of serum samples for ascorbic acid (AA). The sensing platform displays an excellent dynamic range for AA concentration within the 0.5 to 10.0  $\mu\text{M}$  range, with a low detection limit of 0.289  $\mu\text{M}$ .<sup>70</sup>





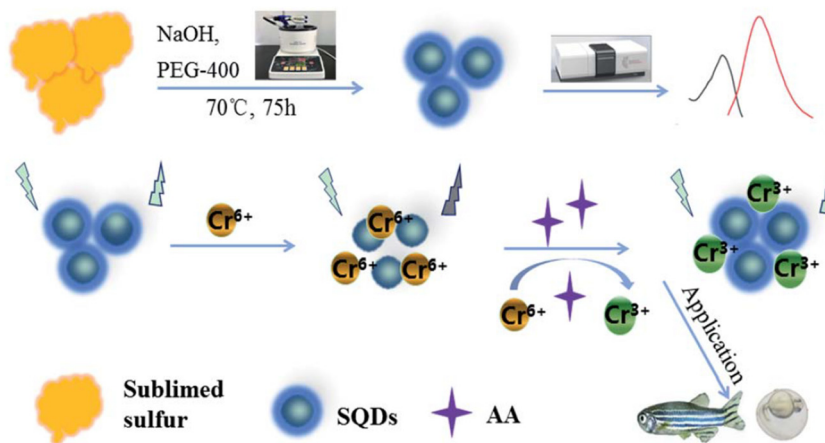


Fig. 2 Schematic illustration of the SQD sensor. From ref. 71 with permission. Copyright 2021, Royal Society of Chemistry.

Fluorescent SQDs were successfully synthesized using sublimed sulfur as the precursor and PEG-400 as the passivator. The presence of Cr(vi) led to a notable decrease in the FL intensity of the SQDs. The addition of ascorbic acid to the SQD/Cr(vi) system resulted in the recovery of the probe's fluorescence, which was attributed to the reduction of Cr(vi) to Cr(III) induced by AA. Consequently, a sequential platform for the detection of Cr(vi) and AA was developed. Under optimized conditions, the FL of SQDs exhibited linear dependencies on the concentrations of Cr(vi) and AA, with a linear range of 0.01–5.5 mM and a detection limit of 3  $\mu\text{M}$ .<sup>71</sup> The recoveries of the probe in human serum were 99.3% and 102.9%, as illustrated in Fig. 2.

Glutathione (GSH) plays crucial roles in biological systems, serving various cellular functions such as maintaining intracellular redox states, detoxification, and metabolism.<sup>55,72,73</sup> Simultaneously, abnormal levels of GSH are linked to numerous clinical diseases, including human immunodeficiency virus (HIV), Parkinson's, liver damage, diabetes, Alzheimer's, inflammatory conditions, and cardiovascular diseases (CVDs).<sup>74,75</sup>

Consequently, the development of sensitive and selective techniques for GSH detection in biological systems is of utmost importance.

In a study conducted by Liu *et al.*, a fluorescence-based assay for detecting GSH was developed, relying on the GSH-modulated quenching effect of Cu<sub>2</sub>O nanoparticles (NPs) on SQDs. The FL of SQDs is efficiently quenched upon the formation of a complex with Cu<sub>2</sub>O NPs through the static quenching effect (SQE). The FL GSH assay exhibits outstanding selectivity and resilience against various interferences and high salt concentrations, facilitating the successful detection of GSH in human blood samples. A noticeable increase in the fluorescence ratio is observed with an elevated concentration of GSH, establishing a linear relationship between the FL ratio and GSH concentration in the range of 20 to 700  $\mu\text{M}$ . The LOD is calculated as 4.0  $\mu\text{M}$ , following the criterion of signal-to-noise ratio of 3 times.<sup>76</sup> As shown in Fig. 3, Han and colleagues identified high-quality sulfur quantum dots (H-SQDs) that exhibited heightened anodic electrochemiluminescence (ECL) emission in a water-based solution. These H-SQDs showcase strong FL

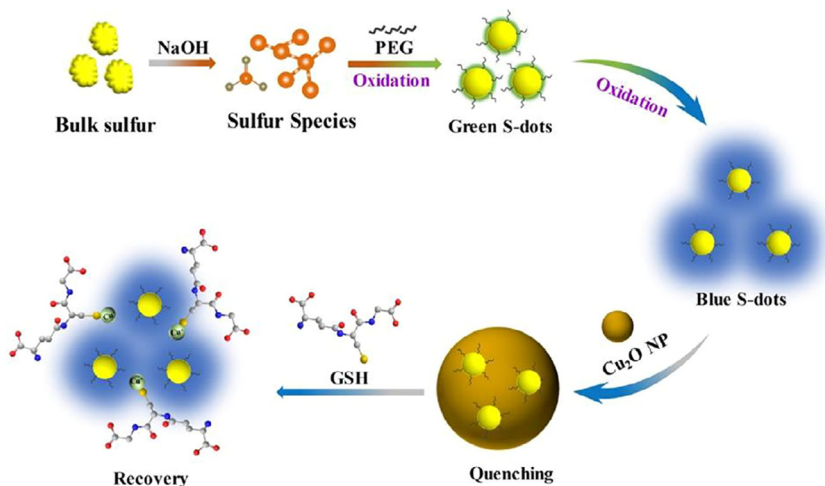


Fig. 3 Schematic illustration of the fluorescence assay for GSH. From ref. 76 with permission. Copyright 2022, Elsevier.



characteristics, facilitating the ultra-trace detection of GSH with an outstanding detection limit of 35 nM.<sup>77</sup>

Alkaline phosphatase (ALP) is a crucial hydrolase in mammalian tissues and plays a vital role in catalyzing the hydrolysis of nucleic acids, proteins, and certain small molecules.<sup>78,79</sup> Due to its significance as an indicator of various diseases such as breast and prostate cancer, bone disorders, liver dysfunction, and diabetes, abnormal expression levels of ALP in serum are considered important diagnostic markers. ALP has, therefore, become a widely utilized enzyme in clinical practice, and its activity is often recognized as a key biomarker for diagnostics.<sup>80,81</sup> Consequently, there is an urgent need to develop a sensitive and straightforward method for monitoring ALP activity to meet the demands of numerous bioanalytical applications.

In this study, Ning *et al.* employed a straightforward approach to synthesize SQDs with excitation and emission wavelengths of 355 nm and 440 nm, respectively. The introduction of ALP into the system resulted in the quenching of the FL intensity of SQDs. These sensor platforms demonstrated high sensitivity and selectivity in detecting ALP, with a linear response observed in the concentration range of 0.25–100 U L<sup>-1</sup> and detection limits of 0.08 and 0.10 U L<sup>-1</sup>, respectively. The sensor platform was effectively applied for sensing ALP in serum samples and monitoring ALP in cells.<sup>82</sup>

In this study, Ma *et al.* utilized a microwave-assisted method with sulfur powder as the precursor to synthesize SQDs. They presented an FL assay designed for the detection of ALP. The FL of the SQDs was initially quenched by Cr(VI). In the presence of ALP, the enzymatic hydrolysis of 2-phospho-L-ascorbic acid catalyzed by ALP produced ascorbic acid. This generated ascorbic acid effectively reduced Cr(VI) to Cr(III), thereby restoring the FL intensity of the SQDs. The FL intensity of the probe demonstrated a dynamic range of 1.5–5.0 U mL<sup>-1</sup>, with a calculated LOD of 0.13 U mL<sup>-1</sup>. The assay showed commendable sensitivity and selectivity and was successful in detecting ALP in serum samples,<sup>83</sup> as shown in Fig. 4.

Dopamine (DA), a naturally occurring neurotransmitter in the brain, significantly impacts the functioning of the central nervous, hormonal, and cardiovascular systems.<sup>84</sup> Variations in blood dopamine levels can serve as indicators for diseases such as Parkinson's, Alzheimer's, and schizophrenia.<sup>85</sup> Given its profound impact on overall health, it is imperative to develop

straightforward and efficient techniques for detecting dopamine in biological samples.

In this study, an extremely sensitive sensor was developed to detect dopamine, employing SQDs as luminescent materials. SQDs were utilized to identify dopamine within the linear range of  $1 \times 10^{-10}$  to  $1 \times 10^{-3}$  M, achieving a detection limit of  $2.5 \times 10^{-11}$  M. This suggested approach is suitable for analyzing real samples and holds the potential for advancing novel lumino-phores, contributing to advancements in human health.<sup>86</sup>

Exploring early indicators of kidney and retinal damage during the initial phase of angiopathy, when widely accepted organ function parameters remain within the normal range, is currently a focal point of extensive global research.<sup>87,88</sup> Numerous studies have highlighted disturbances in glycoprotein and glycosaminoglycan metabolism, including the involvement of the *N*-acetyl-beta-D-glucosaminidase (NAG) enzyme, as a contributing factor to diabetic retinopathy and nephropathy.<sup>89,90</sup> Hence, there is a pressing need to develop a more refined method for detecting NAG with increased sensitivity.

Jiixin and colleagues devised a fluorescent sensor utilizing polyethylene glycol (400) (PEG-400)-modified SQDs subjected to H<sub>2</sub>O<sub>2</sub>-assisted etching. Leveraging the FL IFE, the FL of SQDs can be suppressed by *p*-nitrophenol (PNP) generated through the *N*-acetyl-beta-D-glucosaminidase (NAG)-catalyzed hydrolysis of *p*-nitrophenyl-*N*-acetyl-beta-D-glucosaminide (PNP-NAG). The SQDs served effectively as a fluorescent probe for detecting NAG activity in the range of 0.4 to 7.5 U L<sup>-1</sup>, with a detection limit of 0.1 U L<sup>-1</sup>. Notably, the method exhibited high selectivity and was successfully employed for detecting NAG activity in serum samples,<sup>91</sup> as shown in Fig. 5.

Uric acid (UA) represents the primary byproduct of purine metabolism within the human body, predominantly found in urine and serum.<sup>92,93</sup> Maintaining a normal level of UA is crucial for overall health, with acceptable ranges in urine and serum spanning from 2.49 to 4.46 mM and 0.13 to 0.46 mM, respectively.<sup>94</sup> Deviations from these normal levels, whether higher or lower, can lead to various health issues such as gout, kidney disease, high blood pressure, elevated blood lipids, atherosclerosis, Parkinson's disease, Alzheimer's disease, and other conditions.<sup>95,96</sup> Consequently, constant monitoring of UA levels in bodily fluids is of utmost importance.

In this investigation, sulfur quantum dots modified with heparin (Hep-SQDs) generated display emissions that were not

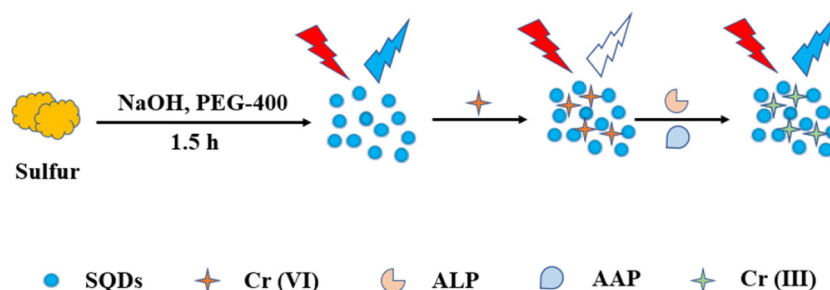


Fig. 4 Schematic diagram of the synthesis of SQDs and determination of ALP. From ref. 83 with permission. Copyright 2022, MDPI.



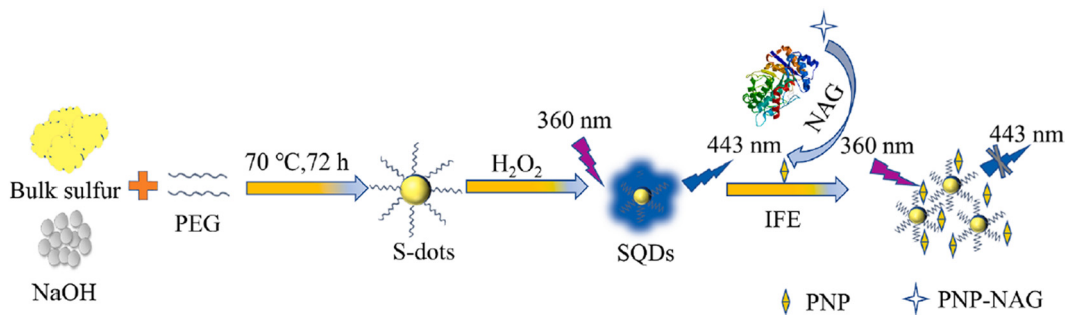


Fig. 5 Schematic diagram for the synthesis of SQDs and its application for NAG. From ref. 91 with permission. Copyright 2023, Elsevier.

dependent on excitation. A ratiometric FL probe utilizing the inner filter effect between the Hep-SQDs and 2,3-diaminophenazine, along with the oxidative product of *o*-phenylenediamine, was used for detecting UA. The proposed probe showed outstanding selectivity and sensitivity for UA analysis, with a detection limit of 0.56  $\mu\text{M}$ . Moreover, this established FL probe was effectively utilized to assess UA levels in human serum,<sup>97</sup> as shown in Fig. 6.

The identification of enzyme activity within the human body is crucial for both clinical diagnosis and biomedical research.<sup>98,99</sup> The activity of lactate dehydrogenase (LDH), a key intermediate in biological systems, is intricately linked to human health. Its correlation with various cancers, such as nasopharyngeal cancer, head and neck cancer, urothelial cancer, bladder cancer, and melanoma, particularly underscores its association with the adverse prognosis of melanoma.<sup>100</sup> Given that these diseases typically result in a significant elevation in LDH concentration in biofluids, such as serum, it is imperative to establish sensitive, convenient, and rapid methods for detecting LDH.

The FL of SQDs produced using the microwave method exhibits a specific enhancement in the presence of nicotinamide

adenine dinucleotide ( $\text{NAD}^+$ ). Exploiting this characteristic, LDH catalyzes the reduction of pyruvate to lactic acid in the presence of reductive coenzyme I (NADH), concurrently transforming NADH into  $\text{NAD}^+$ . This transformation distinctly amplifies the FL intensity of the SQDs. By leveraging the increase in FL intensity, the assay enables the detection of LDH within the range of 500–40 000  $\text{U L}^{-1}$ , with an LOD of 262  $\text{U L}^{-1}$ . Successfully applied to detect LDH activity in serum, the assay demonstrates promising potential for clinical applications,<sup>101</sup> as depicted in Fig. 7.

Butyrylcholinesterase (BChE) is an enzyme with non-specific cholinesterase properties capable of breaking down choline-based esters.<sup>102</sup> It is synthesized in the human liver and swiftly released into the bloodstream, contributing to cholinesterase activity in human serum.<sup>103</sup> The expression level of BChE in human serum serves as a crucial indicator in the clinical diagnosis of various conditions such as organophosphate toxicity, liver dysfunction, poststroke dementia, and Alzheimer's disease.<sup>104,105</sup> Among conventional methods, fluorescence detection stands out for its high sensitivity, cost-effectiveness, and efficiency in screening for BChE in biological samples.

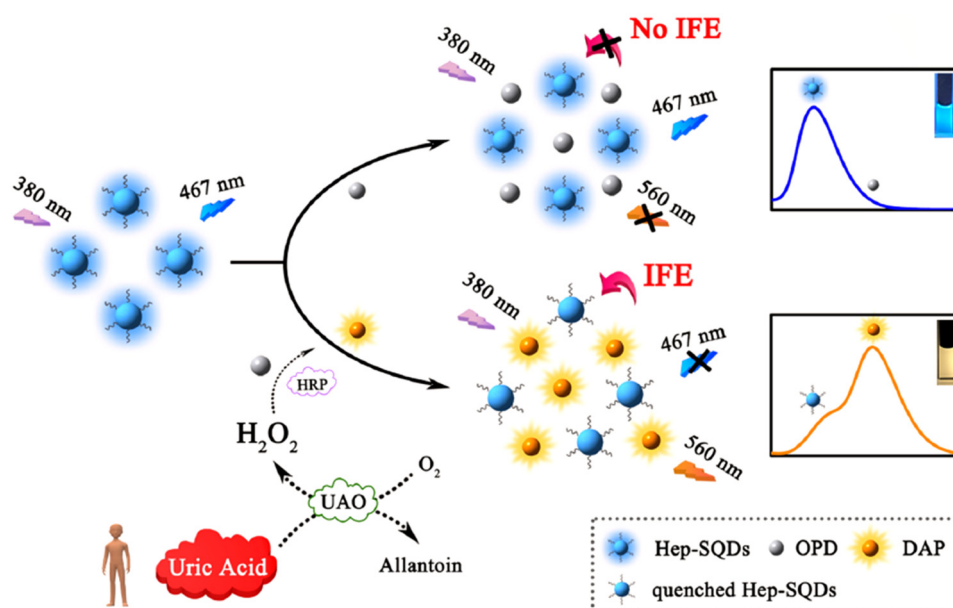


Fig. 6 Diagram depicting the probe design using Hep-SQDs for the assessment of UA. From ref. 97 with permission. Copyright 2022, Elsevier.



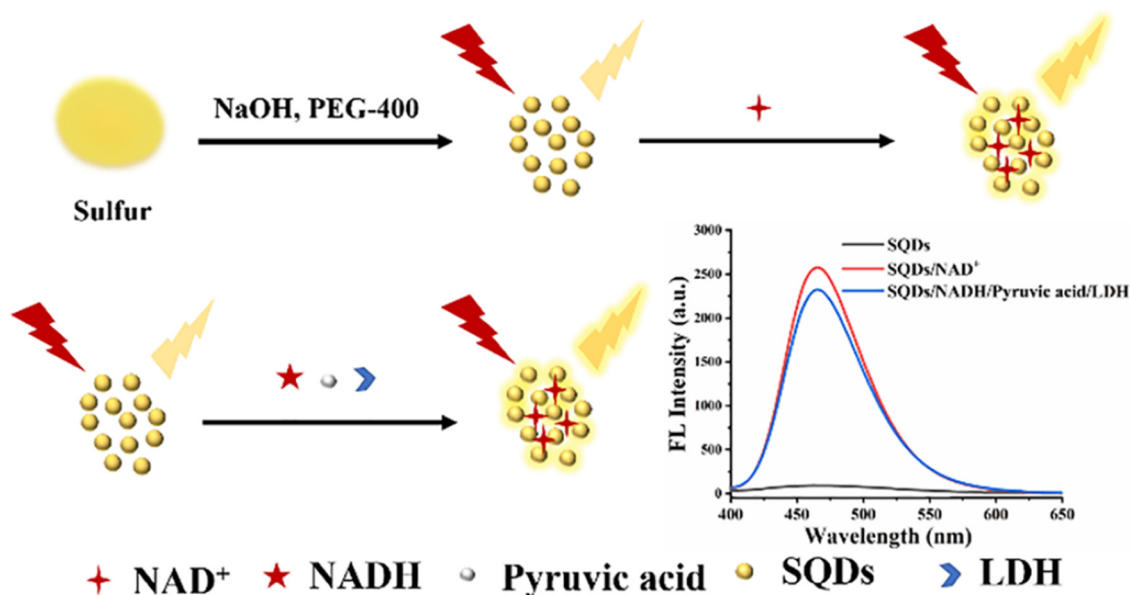


Fig. 7 Schematic illustration of LDH detection. From ref. 101 with permission. Copyright 2022, Elsevier.

Ma and colleagues<sup>106</sup> developed a ratiometric FL assay.  $\text{MnO}_2$  nanosheets were utilized to quench the FL of blue-emissive S-dots and amplify the FL of yellow-emissive OPD by catalyzing their oxidation reactions. A linear correlation was established between the intensity ratio of blue to yellow and BChE concentration within the range of 30–500  $\text{U L}^{-1}$ , with a calculated limit of detection of 17.8  $\text{U L}^{-1}$ . The ratiometric FL assay demonstrated exceptional selectivity for acetylcholinesterase and tolerance to various other species. The developed method demonstrated a robust detection performance in human serum and inhibitor screening, as illustrated in Fig. 8.

A new investigation introduced a highly responsive fluorescence assay to assess the BChE activity. This approach leverages the self-polymerization-modulated FL of SQDs. The assessment of BChE levels is conducted through the evaluation of the restored FL of SQDs, highlighting a consistent correlation

between the FL ratio and BChE concentration within the 0.01–10  $\text{U L}^{-1}$  range. The determined limit of detection is exceptionally low at 0.0069  $\text{U L}^{-1}$ , establishing a new record as the lowest reported value to date. These features facilitate the direct evaluation of BChE activity in serum.<sup>107</sup>

Zoledronic acid (ZA) is a third-generation bisphosphonate with a heterocyclic imidazole structure. It induces apoptosis in osteoclast cells by inhibiting farnesyl pyrophosphate synthase, a crucial enzyme involved in protein prenylation.<sup>108</sup> This enzyme plays a key role in regulating the proliferation of human tumor cells. Numerous preclinical studies have confirmed that nitrogen-containing bisphosphonates, particularly ZA, exert direct antitumor effects, particularly in human breast cancer cell lines. These effects are attributed to the reduction of tumor cell proliferation and the subsequent promotion of apoptosis *in vitro*.<sup>109,110</sup>

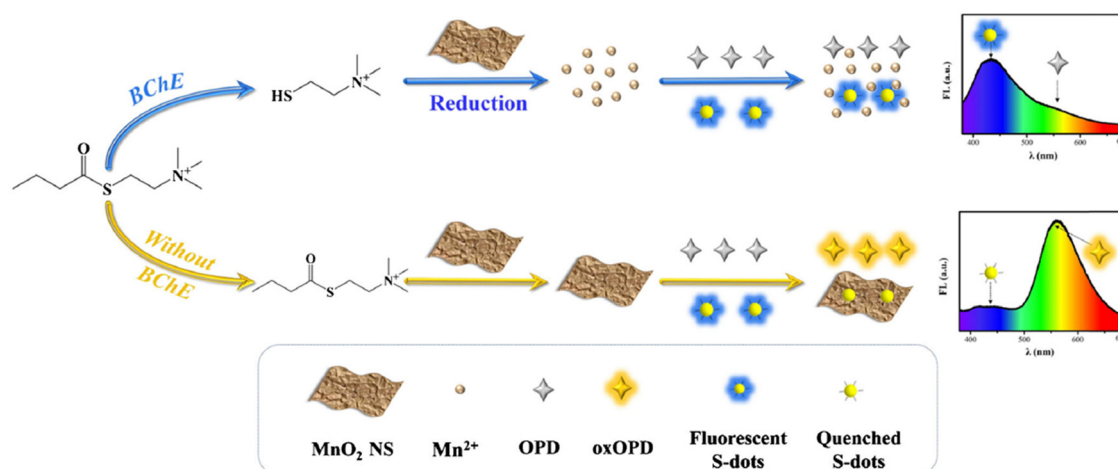


Fig. 8 Schematic illustration of the assay for the detection of BChE. From ref. 106 with permission. Copyright 2021, Springer.





The administration of ZA to cancer patients with bone metastases typically involves intravenous or transdermal injections. Given its accumulation primarily in the bone mineral matrix, it is essential to accurately assess the pharmacokinetics and toxic effects of ZA in body fluids such as urine and plasma.<sup>111</sup> Therefore, there is a critical need to develop sensitive, quantitative analytical methods for the precise evaluation of this drug.<sup>112</sup> To address this, it is imperative to create intelligent fluorescent probes that enable rapid and selective detection of ZA.

In the year 2022, Tan and colleagues demonstrated the use of Fe<sup>3+</sup>-mediated fluorescent SQDs as a probe. These SQDs, emitting blue light, were effectively utilized for detecting ZA in various samples such as human serum, urine, and drugs, providing a convenient application method. The analysis of ZA in diverse samples indicated linear detection regions within the concentration range of 5–200 μM, with a detection limit as low as 1.7 μM.<sup>113</sup>

Norfloxacin (NFX), a member of the fluoroquinolone family, is a fully synthetic antibiotic. Currently, it is extensively employed in animal husbandry and aquaculture for the prevention and treatment of specific infectious diseases.<sup>114</sup> However, excessive norfloxacin residues are present in both the environment and food sources. This surplus residue poses potential risks to human health, including complications such as kidney disease, allergic reactions, reproductive system disorders, and even cancer.<sup>115,116</sup> Therefore, it is crucial to develop a rapid, precise, and reliable method for monitoring NFX residues in biological samples.

Wang and colleagues conducted a distinctive study showing remarkably low detection limits of  $3.3 \times 10^{-6}$  M and a linear detection range of 0 to  $2 \times 10^{-4}$  M for the detection of norfloxacin using fluorescent SQDs. In their research, the recovery rate for norfloxacin in human urine ranged from 93.2% to 106.6%.<sup>43</sup>

Research studies on SQDs for small molecule sensing are summarized in Table 1.

**4.1.2. Temperature sensing.** Temperature is one of the fundamental physical quantities capable of representing various chemical or physical phenomena and is important in

human existence.<sup>117,118</sup> In nanomedicine, temperature sensing serves as a crucial diagnostic tool. Consequently, high-precision temperature detection is indispensable in various aspects of life, education, production, and research.<sup>119</sup> Therefore, temperature measurement is crucial for biomedical detection.

Lei *et al.* recently engineered temperature-sensing probes using polyvinyl alcohol (PVA)-capped SQDs *via* a one-pot synthesis strategy. The study demonstrated a gradual decrease in the fluorescence intensity of SQD dispersions as the environmental temperature increased, enabling the detection of temperature variations within the range of 285–335 K with an absolute linear response ( $R^2 = 0.9992$ ). Notably, this research highlights a temperature sensitivity of 0.75%/K for these PVA-capped SQDs. Given their small size, favorable biocompatibility, and temperature-dependent FL, the investigation explored their utility as nanothermometers for monitoring cell temperature,<sup>65</sup> as shown in Fig. 9.

#### 4.2. Pharmaceutical sensing

Pharmaceuticals encompass a category of organic compounds created specifically for their medicinal properties and can serve as drugs to treat various illnesses. Their utilization has significantly contributed to enhancing both human longevity and overall health. The introduction of pharmaceutical innovations since 1940 has played a pivotal role in the remarkable increase in life expectancy.<sup>29,120</sup> SQDs exhibit robust fluorescence and low toxicity, making them well-suited as fluorescence-sensing probes for pharmaceutical drugs.

Nimesulide (Nim), classified as a non-steroidal anti-inflammatory drug,<sup>121</sup> demonstrates effectiveness in addressing conditions such as chronic rheumatoid arthritis, inflammation of the genitourinary system, otorhinolaryngological diseases, odontostomatological practices, and postoperative pain.<sup>122,123</sup> Due to these therapeutic properties, nimesulide is extensively utilized in clinical settings. Therefore, the detection of nimesulide in drug samples is of significant importance.

Recently, Ma *et al.* introduced a synthesis method for L-cysteine-capped SQDs (Cys-SQDs) to facilitate their formation, demonstrating their utility in the fluorescent sensing of Nim. The resulting Cys-SQDs not only served effectively as a

**Table 1** Selected SQDs for different small molecule detections, including targets, synthesis methods, QY, LOD, and dynamic range values

| Target                          | Synthesis method                                | QY     | LOD                             | Dynamic range                               | Ref. |
|---------------------------------|---|--------|---------------------------------|---|------|
| Ascorbic acid                   | Ultrasound-microwave                            | 58.6%  | 0.289 μM                        | 0.5–10.0 μM                                 | 70   |
| Ascorbic acid                   | Assembling-fission                              | —      | 3 μM                            | 0.01–5.5 mM                                 | 71   |
| Glutathione                     | Bubbling-assisted                               | 8%     | 4.0 μM                          | 20–700 μM                                   | 76   |
| Glutathione                     | Post-synthetic etching                          | —      | 35 nM                           | 0–20 μM                                     | 77   |
| Alkaline phosphatase            | H <sub>2</sub> O <sub>2</sub> -assisted         | —      | 0.08 and 0.10 U L <sup>-1</sup> | 0.25–100 U L <sup>-1</sup>                  | 82   |
| Alkaline phosphatase            | Microwave-assisted                              | —      | 0.13 U mL <sup>-1</sup>         | 1.5–5.0 U mL <sup>-1</sup>                  | 83   |
| Dopamine                        | Hydrothermal                                    | —      | $2.5 \times 10^{-11}$ M         | $1 \times 10^{-10}$ to $1 \times 10^{-3}$ M | 86   |
| N-Acetyl-beta-D-glucosaminidase | H <sub>2</sub> O <sub>2</sub> -assisted etching | 18.77% | 0.1 U L <sup>-1</sup>           | 0.4–7.5 U L <sup>-1</sup>                   | 91   |
| Uric acid                       | Bubbling-assisted                               | 11.4%  | 0.56 μM                         | 1–10 μM                                     | 97   |
| Lactate dehydrogenase           | Bubbling-assisted                               | —      | 262 U L <sup>-1</sup>           | 500–40 000 U L <sup>-1</sup>                | 101  |
| Butyrylcholinesterase           | Bubbling-assisted                               | —      | 17.8 U L <sup>-1</sup>          | 30–500 U L <sup>-1</sup>                    | 106  |
| Butyrylcholinesterase           | Bubbling-assisted                               | —      | U L <sup>-1</sup>               | 0.01–10 U L <sup>-1</sup>                   | 107  |
| Zoledronic acid                 | Bubbling-assisted                               | 31.7%  | 1.7 μM                          | 5–200 μM                                    | 113  |
| Norfloxacin                     | Assemble-fission                                | —      | $3.3 \times 10^{-6}$ M          | 0–2 × 10 <sup>-4</sup> M                    | 43   |



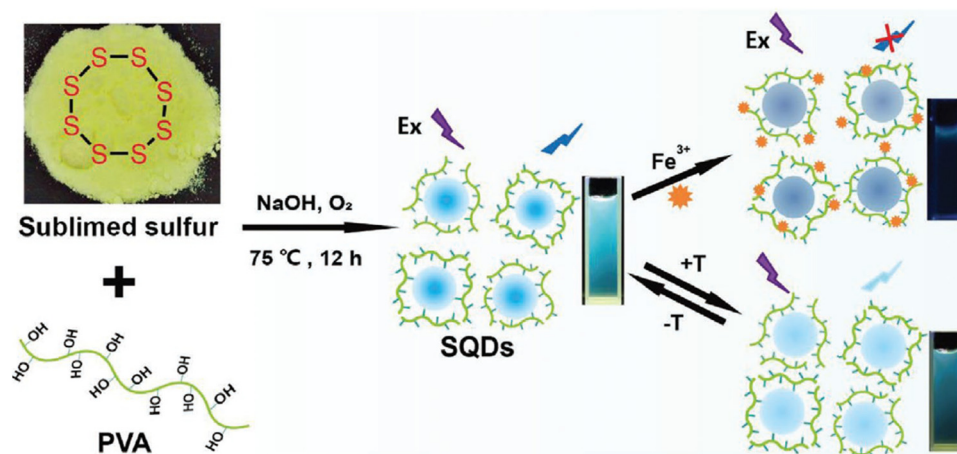


Fig. 9 Schematic illustration of the preparation of the fluorescent probe for temperature. From ref. 65 with permission. Copyright 2021, Wiley.

nanoprobe for Nim detection but also exhibited accurate identification of intracellular Nim with excellent imaging capabilities. Ma *et al.* achieved detection limits of approximately 160 nM for Nim using this nanoprobe, presenting competitive values compared to the currently employed sensing probes. Nim was successfully detected in tablet form, and the Nim content in the diluted tablet measurement solution was measured at 8.59  $\mu$ M. Quantitative spike recoveries for Nim determination in practical samples ranged from 93.23% to 110.01%, with relative standard deviations (RSDs) between 0.78% and 5.68%,<sup>124</sup> as shown in Fig. 10.

Antibiotics such as cloquinol (CQ) play a crucial role in addressing a diverse range of microbial infections.<sup>125</sup> CQ,

classified as a hydroxyquinoline, impedes the activity of enzymes essential for DNA replication. This medication has demonstrated efficacy against viral and protozoal infections. In the treatment of skin infections, topical formulations of CQ are employed due to their potent antifungal and antiprotozoal properties.<sup>126</sup> Additionally, CQ has found applications in various pharmacological contexts, including the treatment of neurological disorders, human prostate cancer, and neurodegenerative conditions such as Huntington's and Parkinson's diseases.<sup>127,128</sup> Consequently, there is a keen interest in developing a low-cost, rapid-response, and user-friendly sensor for the accurate quantification of CQ.

In this context, the FL enhancement effect of Zn<sup>2+</sup> on the SQDs was not particularly pronounced; however, a notable

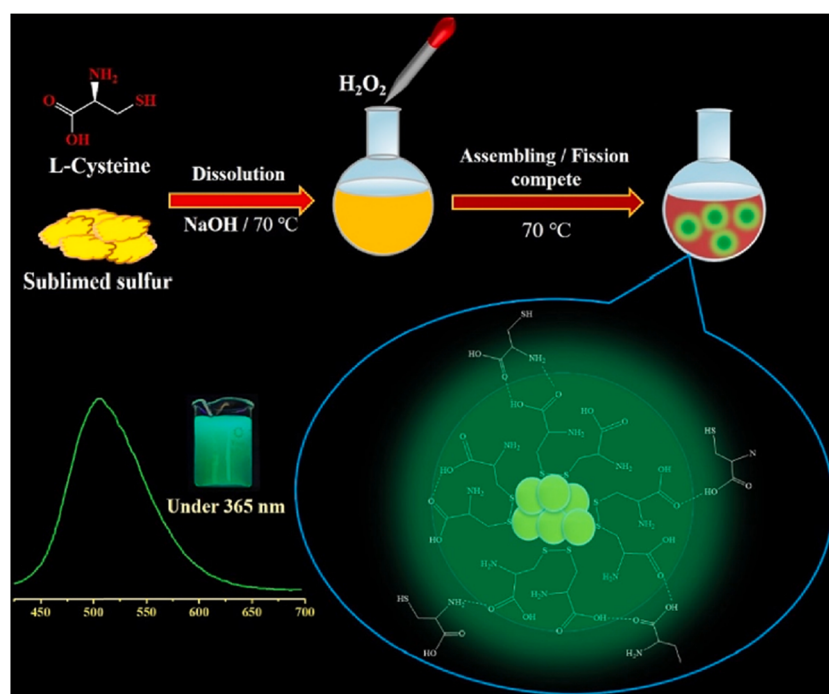


Fig. 10 Schematic diagram of the synthetic procedure for the probe for Nim. From ref. 124 with permission. Copyright 2023, Elsevier.



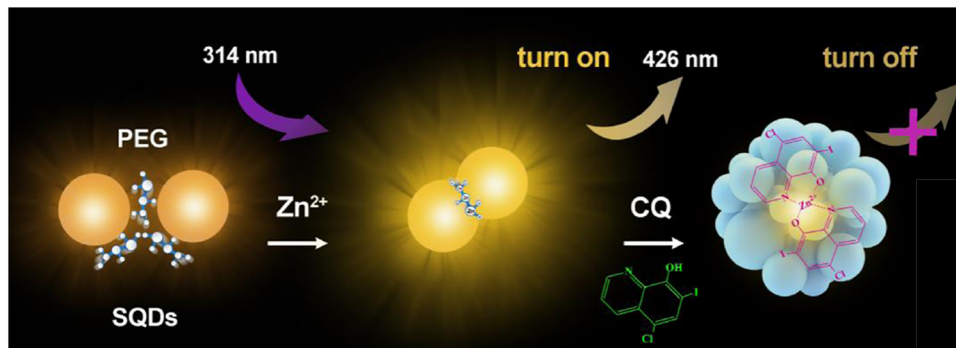


Fig. 11 Schematic of the fluorometric assay for CQ. From ref. 129 with permission. Copyright 2020, Springer.

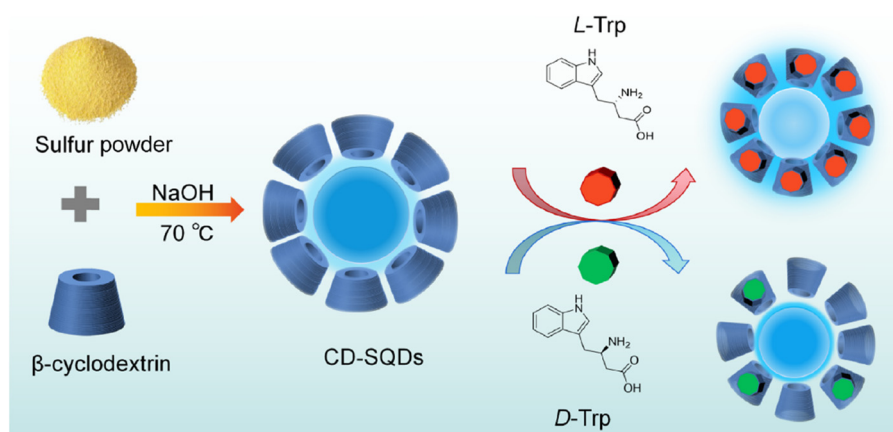


Fig. 12 Schematic illustration of the sensing of L and D-Trp. From ref. 132 with permission. Copyright 2023, American Chemical Society.

quenching modulation effect was observed in the presence of CQ. Consequently, this led to an expanded linear analytical range by two orders of magnitude (from 0.024–0.24  $\mu\text{M}$  and 0.62–30  $\mu\text{M}$ ), with a limit of detection of 0.015  $\mu\text{M}$ . For practical applications, precise weighing of commercially available CQ cream samples has been undertaken,<sup>129</sup> as shown in Fig. 11.

Tryptophan (Trp), an essential amino acid crucial for protein and peptide metabolism in the human body, plays a vital role in establishing and maintaining nitrogen balance in the diet.<sup>130</sup> Additionally, tryptophan is important in the nervous system.<sup>131</sup> Since the human body cannot synthesize tryptophan, it must be obtained *via* tablets. Therefore, there is a critical need to develop a straightforward, easy-to-use, low-toxicity, and highly efficient analytical method for detecting tryptophan, especially under various drug-related conditions.

A sensing platform utilizing sulfur quantum dots coated with  $\beta$ -cyclodextrin (CD-SQDs) was developed for the selective FL recognition of Trp enantiomers. Consequently, the FL

response of the CD-SQDs varies between L-Trp and D-Trp. Experimental validation using an actual sample of a compound amino acid injection demonstrated the effective recognition of L-Trp by the CD-SQD sensor. The detection system for L-Trp exhibited a linear range of 10 to 500 nM, with an LOD of 2.3 nM. The verification and practical application of CD-SQDs for the quantitative sensing of L-Trp were conducted using real samples of compound amino acid injection,<sup>132</sup> as illustrated in Fig. 12.

Research studies of SQDs for pharmaceutical drug sensing are summarized in Table 2.

## 5. Challenges

In spite of substantial advancements in this domain, certain challenges must be more thoroughly addressed in the synthesis and design of probes based on sulfur quantum dots.

Table 2 Selected SQDs for different pharmaceutical drug detections, including targets, synthesis methods, QY, LOD, and dynamic range values

| Target     | Synthesis method  | QY     | LOD                 | Dynamic range                                      | Ref. |
|------------|-------------------|--------|---------------------|--|------|
| Nimesulide | Bubbling-assisted | 10.50% | 160 nM              | 0–100 $\mu\text{M}$                                | 124  |
| Clioquinol | Hydrothermal      | 0.67%  | 0.015 $\mu\text{M}$ | 0.024–0.24 $\mu\text{M}$ and 0.62–30 $\mu\text{M}$ | 129  |
| Tryptophan | Hydrothermal      | 0.016  | 2.3 nM              | 10–500 nM  | 132  |



These challenges include the design of fluorescent probes with high quantum yields, exceptional emissive properties, and superior stability. Additionally, there is a need for extensive clinical testing and precautions when handling biological samples and pharmaceutical drugs, particularly in the context of specific diseases.

## 6. Conclusion

Chemists are interested in fluorescence-based sensors for various chemical species due to their cost-effectiveness and rapid response. This review delves into the role of SQDs in this realm, capitalizing on their advantages, such as unique composition, compact size, and minimal toxicity, rendering them efficient sensors for diverse molecular species and drugs. However, there is still potential for further improvements in sensors that rely on the fluorescence detection of these substances. Ongoing efforts are crucial for developing novel SQD sensors capable of identifying various chemical species in biological and pharmaceutical samples. It is now an opportune moment to transition to a universal system for preparation, one that can be scaled up for industrial production and paves the way for SQD-based bioanalysis and pharmaceutical applications with superior sensing capabilities. Undoubtedly, SQDs are promising materials for various applications and are poised to play vital roles in numerous other applications in the near future.

## 7. Future perspectives

This review explores the broadened applications of SQDs as fluorescent probes for detecting targets in human serum and drug samples. A key contribution of our work is to present this undertaking as a valuable source of data, providing researchers with insights and encouraging further exploration in the field of FL sensing, specifically through the utilization of SQDs.

- Natural resources can be utilized in the synthesis of SQDs to enhance their luminescence properties and achieve a higher quantum yield.
- The fabrication of SQDs for ion sensing in biological samples continues to present notable challenges, even in the recent era.
- Modification of the precursors of SQDs results in improved luminescence properties. The utilization of novel, biodegradable, and non-toxic reagents offers the potential for the detection of a broad range of analytes in different samples.

## Data availability

Data sharing is not applicable to this article as no datasets were generated or analysed during the current study.

## Conflicts of interest

There are no conflicts to declare.

## Acknowledgements

K. F. K. extends special thanks to the University of Sulaimani, College of Science, and the Chemistry Department for all of their cooperation.

## References

- 1 Z. L. Wu, Z. X. Liu and Y. H. Yuan, Carbon dots: Materials, synthesis, properties and approaches to long-wavelength and multicolor emission, *J. Mater. Chem. B*, 2017, 5(21), 3794–3809, DOI: [10.1039/c7tb00363c](https://doi.org/10.1039/c7tb00363c).
- 2 X. Hai, Q. X. Mao, W. J. Wang, X. F. Wang, X. W. Chen and J. H. Wang, An acid-free microwave approach to prepare highly luminescent boron-doped graphene quantum dots for cell imaging, *J. Mater. Chem. B*, 2015, 3(47), 9109–9114, DOI: [10.1039/c5tb01954k](https://doi.org/10.1039/c5tb01954k).
- 3 R. Mohammadi, *et al.*, Fluorescence sensing and imaging with carbon-based quantum dots for early diagnosis of cancer: A review, *J. Pharm. Biomed. Anal.*, 2022, 212, 114628, DOI: [10.1016/j.jpba.2022.114628](https://doi.org/10.1016/j.jpba.2022.114628).
- 4 K. F. Kayani and C. N. Abdullah, A Dual-Mode Detection Sensor Based on Nitrogen-Doped Carbon Dots for Visual Detection of Fe(III) and Ascorbic Acid *via* a Smartphone, *J. Fluoresc.*, 2024, DOI: [10.1007/s10895-024-03604-0](https://doi.org/10.1007/s10895-024-03604-0).
- 5 S. Y. Lim, W. Shen and Z. Gao, Carbon quantum dots and their applications, *Chem. Soc. Rev.*, 2015, 44(1), 362–381, DOI: [10.1039/c4cs00269e](https://doi.org/10.1039/c4cs00269e).
- 6 E. Porret, X. Le Guével and J. L. Coll, Gold nanoclusters for biomedical applications: Toward: In vivo studies, *J. Mater. Chem. B*, 2020, 8(11), 2216–2232, DOI: [10.1039/c9tb02767j](https://doi.org/10.1039/c9tb02767j).
- 7 I. Chakraborty and T. Pradeep, Atomically Precise Clusters of Noble Metals: Emerging Link between Atoms and Nanoparticles, *Chem. Rev.*, 2017, 117(12), 8208–8271, DOI: [10.1021/acs.chemrev.6b00769](https://doi.org/10.1021/acs.chemrev.6b00769).
- 8 H. Wang, J. Lai, X. Xu, W. Yu and X. Wang, Combination of gold nanoclusters and silicon quantum dots for ratiometric fluorometry: One system, two mechanisms, *J. Pharm. Biomed. Anal.*, 2024, 240, 115940, DOI: [10.1016/j.jpba.2023.115940](https://doi.org/10.1016/j.jpba.2023.115940).
- 9 J. Yang and X. Zhong, CdTe based quantum dot sensitized solar cells with efficiency exceeding 7% fabricated from quantum dots prepared in aqueous media, *J. Mater. Chem. A*, 2016, 4(42), 16553–16561, DOI: [10.1039/c6ta07399a](https://doi.org/10.1039/c6ta07399a).
- 10 R. Blonder, The story of nanomaterials in modern technology: An advanced course for chemistry teachers, *J. Chem. Educ.*, 2011, 88(1), 49–52, DOI: [10.1021/ed100614f](https://doi.org/10.1021/ed100614f).
- 11 E. M. Boatman, G. C. Lisensky and K. J. Nordell, A safer, easier, faster synthesis for CdSe quantum dot nanocrystals, *J. Chem. Educ.*, 2005, 82(11), 1697–1699, DOI: [10.1021/ed082p1697](https://doi.org/10.1021/ed082p1697).
- 12 S. Das, H. Mazumdar, K. R. Khondakar, A. K. Kaushik and Y. K. Mishra, Quantum Biosensors: Principles and Applications in Medical Diagnostics, *ECS Sensors Plus*, 2024, 3(2), 1–13, DOI: [10.1149/2754-2726/ad47e2](https://doi.org/10.1149/2754-2726/ad47e2).





- 13 V. Chugh, A. Basu, N. K. Kaushik, A. Kaushik, Y. K. Mishra and A. K. Basu, Smart nanomaterials to support quantum-sensing electronics, *Mater. Today Electron.*, 2023, **6**, 100067, DOI: [10.1016/j.mtelec.2023.100067](https://doi.org/10.1016/j.mtelec.2023.100067).
- 14 U. Resch-Genger, M. Grabolle, S. Cavaliere-Jaricot, R. Nitschke and T. Nann, Quantum dots versus organic dyes as fluorescent labels, *Nat. Methods*, 2008, **5**(9), 763–775, DOI: [10.1038/nmeth.1248](https://doi.org/10.1038/nmeth.1248).
- 15 D. A. Kader, *et al.*, Green synthesis of ZnO/catechin nanocomposite: Comprehensive characterization, optical study, computational analysis, biological applications and molecular docking, *Mater. Chem. Phys.*, 2024, **319**, 129408, DOI: [10.1016/j.MATCHEMPHYS.2024.129408](https://doi.org/10.1016/j.MATCHEMPHYS.2024.129408).
- 16 J. Shen, Y. Zhu, X. Yang and C. Li, Graphene quantum dots: Emergent nanolights for bioimaging, sensors, catalysis and photovoltaic devices, *Chem. Commun.*, 2012, **48**(31), 3686–3699, DOI: [10.1039/c2cc00110a](https://doi.org/10.1039/c2cc00110a).
- 17 O. B. A. Shatery, K. F. Kayani, M. S. Mustafa and S. J. Mohammed, Rational design for enhancing sensitivity and robustness of a probe *via* encapsulation of carbon dots into a zeolitic imidazolate framework-8 for quantification of tetracycline in milk with greenness evaluation, *Res. Chem. Intermed.*, 2024, **50**, 2291–2306, DOI: [10.1007/s11164-024-05271-z](https://doi.org/10.1007/s11164-024-05271-z).
- 18 K. F. Kayani, M. K. Rahim, S. J. Mohammed, H. R. Ahmed, M. S. Mustafa and S. B. Aziz, Recent Progress in Folic Acid Detection Based on Fluorescent Carbon Dots as Sensors: A Review, *J. Fluoresc.*, 2024, DOI: [10.1007/s10895-024-03728-3](https://doi.org/10.1007/s10895-024-03728-3).
- 19 K. F. Kayani, O. B. A. Shatery, M. S. Mustafa, A. H. Alshatteri, S. J. Mohammed and S. B. Aziz, Environmentally sustainable synthesis of whey-based carbon dots for ferric ion detection in human serum and water samples: evaluating the greenness of the method, *RSC Adv.*, 2024, **14**(8), 5012–5021, DOI: [10.1039/d3ra08680a](https://doi.org/10.1039/d3ra08680a).
- 20 D. Sun, T. Liu, S. Li, C. Wang and K. Zhuo, Preparation and application of carbon dots with tunable luminescence by controlling surface functionalization, *Opt. Mater.*, 2020, **108**, 110450, DOI: [10.1016/j.optmat.2020.110450](https://doi.org/10.1016/j.optmat.2020.110450).
- 21 M. Li, T. Chen, J. J. Gooding and J. Liu, Review of carbon and graphene quantum dots for sensing, *ACS Sens.*, 2019, **4**(7), 1732–1748, DOI: [10.1021/acssensors.9b00514](https://doi.org/10.1021/acssensors.9b00514).
- 22 V. C. Hoang, K. Dave and V. G. Gomes, Carbon quantum dot-based composites for energy storage and electrocatalysis: Mechanism, applications and future prospects, *Nano Energy*, 2019, **66**, 104093, DOI: [10.1016/j.nanoen.2019.104093](https://doi.org/10.1016/j.nanoen.2019.104093).
- 23 D. Iannazzo, I. Ziccarelli and A. Pistone, Graphene quantum dots: Multifunctional nanoplatfoms for anticancer therapy, *J. Mater. Chem. B*, 2017, **5**(32), 6471–6489, DOI: [10.1039/c7tb00747g](https://doi.org/10.1039/c7tb00747g).
- 24 L. Dai, Carbon-based catalysts for metal-free electrocatalysis, *Curr. Opin. Electrochem.*, 2017, **4**(1), 18–25, DOI: [10.1016/j.coelec.2017.06.004](https://doi.org/10.1016/j.coelec.2017.06.004).
- 25 M. X. Zhao and B. J. Zhu, The Research and Applications of Quantum Dots as Nano-Carriers for Targeted Drug Delivery and Cancer Therapy, *Nanoscale Res. Lett.*, 2016, **11**(1), 207, DOI: [10.1186/s11671-016-1394-9](https://doi.org/10.1186/s11671-016-1394-9).
- 26 M. Pan, X. Xie, K. Liu, J. Yang, L. Hong and S. Wang, Fluorescent carbon quantum dots-synthesis, functionalization and sensing application in food analysis, *Nanomaterials*, 2020, **10**(5), 1–25, DOI: [10.3390/nano10050930](https://doi.org/10.3390/nano10050930).
- 27 H. Bai, Z. Tu, Y. Liu, Q. Tai, Z. Guo and S. Liu, Dual-emission carbon dots-stabilized copper nanoclusters for ratiometric and visual detection of Cr<sup>2+</sup> ions and Cd<sup>2+</sup> ions, *J. Hazard. Mater.*, 2020, **386**, 121654, DOI: [10.1016/j.jhazmat.2019.121654](https://doi.org/10.1016/j.jhazmat.2019.121654).
- 28 S. Zhu, Y. Song, X. Zhao, J. Shao, J. Zhang and B. Yang, The photoluminescence mechanism in carbon dots (graphene quantum dots, carbon nanodots, and polymer dots): current state and future perspective, *Nano Res.*, 2015, **8**(2), 355–381, DOI: [10.1007/s12274-014-0644-3](https://doi.org/10.1007/s12274-014-0644-3).
- 29 K. F. Kayani and K. M. Omer, A red luminescent europium metal organic framework (Eu-MOF) integrated with a paper strip using smartphone visual detection for determination of folic acid in pharmaceutical formulations, *New J. Chem.*, 2022, **46**(17), 8152–8161, DOI: [10.1039/d2nj00601d](https://doi.org/10.1039/d2nj00601d).
- 30 K. F. Kayani, S. J. Mohammed, N. N. Mohammad, G. H. Abdullah, D. A. Kader and N. S. Hamad Mustafa, Ratiometric fluorescence detection of tetracycline in milk and tap water with smartphone assistance for visual pH sensing using innovative dual-emissive phosphorus-doped carbon dots, *Food Control*, 2024, **164**, 110611, DOI: [10.1016/j.FOODCONT.2024.110611](https://doi.org/10.1016/j.FOODCONT.2024.110611).
- 31 F. Arshad, M. P. Sk, S. K. Maurya and H. R. Siddique, Mechanochemical Synthesis of Sulfur Quantum Dots for Cellular Imaging, *ACS Appl. Nano Mater.*, 2021, **4**(4), 3339–3344, DOI: [10.1021/acsanm.1c00509](https://doi.org/10.1021/acsanm.1c00509).
- 32 Y. E. Shi, P. Zhang, D. Yang and Z. Wang, Synthesis, photoluminescence properties and sensing applications of luminescent sulfur nanodots, *Chem. Commun.*, 2020, **56**(75), 10982–10988, DOI: [10.1039/d0cc04341a](https://doi.org/10.1039/d0cc04341a).
- 33 Z. Sun, *et al.*, From the perspective of high-throughput recognition: Sulfur quantum dots-based multi-channel sensing platform for metal ions detection, *Chem. Eng. J.*, 2023, **452**(P4), 139594, DOI: [10.1016/j.cej.2022.139594](https://doi.org/10.1016/j.cej.2022.139594).
- 34 J. J. Griebel, R. S. Glass, K. Char and J. Pyun, Polymerizations with elemental sulfur: A novel route to high sulfur content polymers for sustainability, energy and defense, *Prog. Polym. Sci.*, 2016, **58**, 90–125, DOI: [10.1016/j.progpolymsci.2016.04.003](https://doi.org/10.1016/j.progpolymsci.2016.04.003).
- 35 J. Lim, J. Pyun and K. Char, Recent approaches for the direct use of elemental sulfur in the synthesis and processing of advanced materials, *Angew. Chem., Int. Ed.*, 2015, **54**(11), 3249–3258, DOI: [10.1002/anie.201409468](https://doi.org/10.1002/anie.201409468).
- 36 P. Gao, G. Wang and L. Zhou, Luminescent Sulfur Quantum Dots: Synthesis, Properties and Potential Applications, *ChemPhotoChem*, 2020, **4**(11), 5235–5244, DOI: [10.1002/cptc.202000158](https://doi.org/10.1002/cptc.202000158).
- 37 S. Li, D. Chen, F. Zheng, H. Zhou, S. Jiang and Y. Wu, Water-soluble and lowly toxic sulphur quantum dots, *Adv. Funct. Mater.*, 2014, **24**(45), 7133–7138, DOI: [10.1002/adfm.201402087](https://doi.org/10.1002/adfm.201402087).



- 38 M. S. Mustafa, N. N. Mohammad, F. H. Radha, K. F. Kayani, H. O. Ghareeb and S. J. Mohammed, Eco-friendly spectrophotometric methods for concurrent analysis of phenol, 2-aminophenol, and 4-aminophenol in ternary mixtures and water samples: assessment of environmental sustainability, *RSC Adv.*, 2024, **14**(23), 16045–16055, DOI: [10.1039/d4ra01094a](https://doi.org/10.1039/d4ra01094a).
- 39 C. Zhang, *et al.*, Ultrasonication-promoted synthesis of luminescent sulfur nano-dots for cellular imaging applications, *Chem. Commun.*, 2019, **55**(86), 13004–13007, DOI: [10.1039/c9cc06586e](https://doi.org/10.1039/c9cc06586e).
- 40 Z. Hu, *et al.*, 49.25% Efficient Cyan Emissive Sulfur Dots-via Microwave-Assisted Route, *RSC Adv.*, 2020, **10**(29), 17266–17269, DOI: [10.1039/d0ra02778b](https://doi.org/10.1039/d0ra02778b).
- 41 Y. Song, J. Tan, G. Wang, P. Gao, J. Lei and L. Zhou, Oxygen accelerated scalable synthesis of highly fluorescent sulfur quantum dots, *Chem. Sci.*, 2020, **11**(3), 772–777, DOI: [10.1039/c9sc05019a](https://doi.org/10.1039/c9sc05019a).
- 42 H. Wang, *et al.*, Hydrogen Peroxide Assisted Synthesis of Highly Luminescent Sulfur Quantum Dots, *Angew. Chem., Int. Ed.*, 2019, **58**(21), 7040–7044, DOI: [10.1002/anie.201902344](https://doi.org/10.1002/anie.201902344).
- 43 S. Wang, X. Bao, B. Gao and M. Li, A novel sulfur quantum dot for the detection of cobalt ions and norfloxacin as a fluorescent 'switch', *Dalton Trans.*, 2019, **48**(23), 8288–8296, DOI: [10.1039/c9dt01186b](https://doi.org/10.1039/c9dt01186b).
- 44 F. Li, *et al.*, Quantum dot white light emitting diodes with high scotopic/photopic ratios, *Opt. Express*, 2017, **25**(18), 21901, DOI: [10.1364/oe.25.021901](https://doi.org/10.1364/oe.25.021901).
- 45 H. Chen, *et al.*, Sulfur dots-graphene nanohybrid: A metal-free electrocatalyst for efficient N<sub>2</sub>-to-NH<sub>3</sub> fixation under ambient conditions, *Chem. Commun.*, 2019, **55**(21), 3152–3155, DOI: [10.1039/c9cc00461k](https://doi.org/10.1039/c9cc00461k).
- 46 G. Qiao *et al.*, *Signal transduction from small particles: Sulfur nanodots featuring mercury sensing, cell entry mechanism and in vitro tracking performance*, Elsevier B.V., 2020, vol. 382.
- 47 C. Wang, *et al.*, Dual Functional Hydrogen Peroxide Boosted One Step Solvothermal Synthesis of Highly Uniform Sulfur Quantum Dots at Elevated Temperature and Their Fluorescent Sensing, *Sens. Actuators, B*, 2021, **344**, 130326, DOI: [10.1016/j.snb.2021.130326](https://doi.org/10.1016/j.snb.2021.130326).
- 48 X. Peng, Y. Wang, Z. Luo, B. Zhang, X. Mei and X. Yang, Facile synthesis of fluorescent sulfur quantum dots for selective detection of p-nitrophenol in water samples, *Microchem. J.*, 2021, **170**, 106735, DOI: [10.1016/j.microc.2021.106735](https://doi.org/10.1016/j.microc.2021.106735).
- 49 D. Chen, S. Li and F. Zheng, Water soluble sulphur quantum dots for selective Ag<sup>+</sup> sensing based on the ion aggregation-induced photoluminescence enhancement, *Anal. Methods*, 2016, **8**(3), 632–636, DOI: [10.1039/c5ay02451j](https://doi.org/10.1039/c5ay02451j).
- 50 L. Shen, *et al.*, Assembling of Sulfur Quantum Dots in Fission of Sublimed Sulfur, *J. Am. Chem. Soc.*, 2018, **140**(25), 7878–7884, DOI: [10.1021/jacs.8b02792](https://doi.org/10.1021/jacs.8b02792).
- 51 H. Ruan and L. Zhou, Synthesis of Fluorescent Sulfur Quantum Dots for Bioimaging and Biosensing, *Front. Bioeng. Biotechnol.*, 2022, **10**, 1–7, DOI: [10.3389/fbioe.2022.909727](https://doi.org/10.3389/fbioe.2022.909727).
- 52 F. Arshad and M. P. Sk, Luminescent Sulfur Quantum Dots for Colorimetric Discrimination of Multiple Metal Ions, *ACS Appl. Nano Mater.*, 2020, **3**(3), 3044–3049, DOI: [10.1021/acsnm.0c00394](https://doi.org/10.1021/acsnm.0c00394).
- 53 R. V. Reji and V. Biju, Rapid and scalable synthesis of sulfur quantum dots through ozone etching: photoluminescence and FRET-mediated Co<sup>2+</sup> sensing, *New J. Chem.*, 2023, **47**(19), 9113–9123, DOI: [10.1039/d2nj06195c](https://doi.org/10.1039/d2nj06195c).
- 54 S. O. Fakayode, *et al.*, Fluorescent chemical sensors: applications in analytical, environmental, forensic, pharmaceutical, biological, and biomedical sample measurement, and clinical diagnosis, *Appl. Spectrosc. Rev.*, 2024, **59**(1), 1–89, DOI: [10.1080/05704928.2023.2177666](https://doi.org/10.1080/05704928.2023.2177666).
- 55 K. F. Kayani, S. J. Mohammed, D. Ghafoor, M. K. Rahim and H. R. Ahmed, Carbon dot as fluorescence sensor for glutathione in human serum samples: a review, *Mater. Adv.*, 2024, 4618–4633, DOI: [10.1039/d4ma00185k](https://doi.org/10.1039/d4ma00185k).
- 56 B. The Huy, D. T. Thangadurai, M. Sharipov, N. Ngoc Nghia, N. Van Cuong and Y. I. Lee, Recent advances in turn off-on fluorescence sensing strategies for sensitive biochemical analysis – A mechanistic approach, *Microchem. J.*, 2022, **179**, 107511, DOI: [10.1016/j.microc.2022.107511](https://doi.org/10.1016/j.microc.2022.107511).
- 57 X. Cai and B. Liu, Aggregation-Induced Emission: Recent Advances in Materials and Biomedical Applications, *Angew. Chem., Int. Ed.*, 2020, **59**(25), 9868–9886, DOI: [10.1002/anie.202000845](https://doi.org/10.1002/anie.202000845).
- 58 A. Kaur, P. Kaur and S. Ahuja, Förster resonance energy transfer (FRET) and applications thereof, *Anal. Methods*, 2020, **12**(46), 5532–5550, DOI: [10.1039/D0AY01961E](https://doi.org/10.1039/D0AY01961E).
- 59 S. Tao, S. Zhu, T. Feng, C. Zheng and B. Yang, Crosslink-Enhanced Emission Effect on Luminescence in Polymers: Advances and Perspectives, *Angew. Chem., Int. Ed.*, 2020, **59**(25), 9826–9840, DOI: [10.1002/anie.201916591](https://doi.org/10.1002/anie.201916591).
- 60 X. Wang, *et al.*, Dual recognition strategy for ultra-sensitive fluorescent detection of Hg<sup>2+</sup> at femto-molar level based on aptamer functionalized sulfur quantum dots, *Arab. J. Chem.*, 2022, **15**(9), 104080, DOI: [10.1016/j.arabjc.2022.104080](https://doi.org/10.1016/j.arabjc.2022.104080).
- 61 L. Li, C. Yang, Y. Li, Y. Nie and X. Tian, Sulfur quantum dot-based portable paper sensors for fluorometric and colorimetric dual-channel detection of cobalt, *J. Mater. Sci.*, 2021, **56**(7), 4782–4796, DOI: [10.1007/s10853-020-05544-z](https://doi.org/10.1007/s10853-020-05544-z).
- 62 C. Lu, *et al.*, A colorimetric and fluorescence dual-signal determination for iron (II) and H<sub>2</sub>O<sub>2</sub> in food based on sulfur quantum dots, *Food Chem.*, 2022, **366**, 130613, DOI: [10.1016/j.foodchem.2021.130613](https://doi.org/10.1016/j.foodchem.2021.130613).
- 63 Z. Wei, *et al.*, Manipulating time-dependent size distribution of sulfur quantum dots and their fluorescence sensing for ascorbic acid, *Dalton Trans.*, 2022, **51**(26), 10290–10297, DOI: [10.1039/d2dt01584f](https://doi.org/10.1039/d2dt01584f).
- 64 K. F. Kayani, N. N. Mohammad, D. A. Kader and S. J. Mohammed, Ratiometric Lanthanide Metal-Organic



- Frameworks (MOFs) for Smartphone-Assisted Visual Detection of Food Contaminants and Water: A Review, *ChemistrySelect*, 2023, **8**(47), 202303472, DOI: [10.1002/slct.202303472](https://doi.org/10.1002/slct.202303472).
- 65 J. Lei, Z. Huang, P. Gao, J. Sun and L. Zhou, Polyvinyl Alcohol Enhanced Fluorescent Sulfur Quantum Dots for Highly Sensitive Detection of Fe<sup>3+</sup> and Temperature in Cells, *Part. Part. Syst. Charact.*, 2021, **38**(4), 1–8, DOI: [10.1002/ppsc.202000332](https://doi.org/10.1002/ppsc.202000332).
- 66 C. Tang, R. Long, X. Tong, Y. Guo, C. Tong and S. Shi, Dual-emission biomass carbon dots for near-infrared ratiometric fluorescence determination and imaging of ascorbic acid, *Microchem. J.*, 2021, **164**, 106000, DOI: [10.1016/j.microc.2021.106000](https://doi.org/10.1016/j.microc.2021.106000).
- 67 R. Liu, *et al.*, Synthesis of glycine-functionalized graphene quantum dots as highly sensitive and selective fluorescent sensor of ascorbic acid in human serum, *Sens. Actuators, B*, 2017, **241**, 644–651, DOI: [10.1016/j.snb.2016.10.096](https://doi.org/10.1016/j.snb.2016.10.096).
- 68 H. Liu, W. Na, Z. Liu, X. Chen and X. Su, A novel turn-on fluorescent strategy for sensing ascorbic acid using graphene quantum dots as fluorescent probe, *Biosens. Bioelectron.*, 2017, **92**, 229–233, DOI: [10.1016/j.bios.2017.02.005](https://doi.org/10.1016/j.bios.2017.02.005).
- 69 S. Zhuo, J. Fang, M. Li, J. Wang, C. Zhu and J. Du, Manganese(II)-doped carbon dots as effective oxidase mimics for sensitive colorimetric determination of ascorbic acid, *Microchim. Acta*, 2019, **186**(12), 1–8, DOI: [10.1007/s00604-019-3887-6](https://doi.org/10.1007/s00604-019-3887-6).
- 70 Y. Sheng, *et al.*, Size-focusing results in highly photoluminescent sulfur quantum dots with a stable emission wavelength, *Nanoscale*, 2021, **13**(4), 2519–2526, DOI: [10.1039/d0nr07251f](https://doi.org/10.1039/d0nr07251f).
- 71 M. Xia, H. Mei, Q. Qian, R. A. Dahlgren, M. Gao and X. Wang, Sulfur quantum dot-based ‘ON-OFF-ON’ fluorescence platform for detection and bioimaging of Cr(VI) and ascorbic acid in complex environmental matrices and biological tissues, *RSC Adv.*, 2021, **11**(18), 10572–10581, DOI: [10.1039/d1ra00401h](https://doi.org/10.1039/d1ra00401h).
- 72 Z. Li, *et al.*, Carbon dots based photoelectrochemical sensors for ultrasensitive detection of glutathione and its applications in probing of myocardial infarction, *Biosens. Bioelectron.*, 2018, **99**, 251–258, DOI: [10.1016/j.bios.2017.07.065](https://doi.org/10.1016/j.bios.2017.07.065).
- 73 S. Gogoi and R. Khan, NIR upconversion characteristics of carbon dots for selective detection of glutathione, *New J. Chem.*, 2018, **42**(8), 6399–6407, DOI: [10.1039/c8nj00567b](https://doi.org/10.1039/c8nj00567b).
- 74 Q. Y. Cai, *et al.*, A rapid fluorescence ‘switch-on’ assay for glutathione detection by using carbon dots-MnO<sub>2</sub> nanocomposites, *Biosens. Bioelectron.*, 2015, **72**, 31–36, DOI: [10.1016/j.bios.2015.04.077](https://doi.org/10.1016/j.bios.2015.04.077).
- 75 X. Chen, J. Bai, G. Yuan, L. Zhang and L. Ren, One-pot preparation of nitrogen-doped carbon dots for sensitive and selective detection of Ag<sup>+</sup> and glutathione, *Microchem. J.*, 2021, **165**, 106156, DOI: [10.1016/j.microc.2021.106156](https://doi.org/10.1016/j.microc.2021.106156).
- 76 S. Liu, *et al.*, Glutathione modulated fluorescence quenching of sulfur quantum dots by Cu<sub>2</sub>O nanoparticles for sensitive assay, *Spectrochim. Acta, Part A*, 2022, **265**, 120365, DOI: [10.1016/j.saa.2021.120365](https://doi.org/10.1016/j.saa.2021.120365).
- 77 T. Han, *et al.*, Boosted anodic electrochemiluminescence from blue-emissive sulfur quantum dots and its bioanalysis of glutathione, *Electrochim. Acta*, 2021, **381**, 138281, DOI: [10.1016/j.electacta.2021.138281](https://doi.org/10.1016/j.electacta.2021.138281).
- 78 X. Niu, K. Ye, L. Wang, Y. Lin and D. Du, A review on emerging principles and strategies for colorimetric and fluorescent detection of alkaline phosphatase activity, *Anal. Chim. Acta*, 2019, **1086**, 29–45, DOI: [10.1016/j.aca.2019.07.068](https://doi.org/10.1016/j.aca.2019.07.068).
- 79 W. Kang, *et al.*, Monitoring the activity and inhibition of alkaline phosphatase *via* quenching and restoration of the fluorescence of carbon dots, *Microchim. Acta*, 2015, **182**(5–6), 1161–1167, DOI: [10.1007/s00604-014-1439-7](https://doi.org/10.1007/s00604-014-1439-7).
- 80 Y. Zhang, Y. Nie, R. Zhu, D. Han, H. Zhao and Z. Li, Nitrogen doped carbon dots for turn-off fluorescent detection of alkaline phosphatase activity based on inner filter effect, *Talanta*, 2019, **204**, 74–81, DOI: [10.1016/j.talanta.2019.05.099](https://doi.org/10.1016/j.talanta.2019.05.099).
- 81 F. Qu, H. Pei, R. Kong, S. Zhu and L. Xia, Novel turn-on fluorescent detection of alkaline phosphatase based on green synthesized carbon dots and MnO<sub>2</sub> nanosheets, *Talanta*, 2017, **165**, 136–142, DOI: [10.1016/j.talanta.2016.11.051](https://doi.org/10.1016/j.talanta.2016.11.051).
- 82 K. Ning, *et al.*, Inner filter effect-based red-shift and fluorescence dual-sensor platforms with sulfur quantum dots for detection and bioimaging of alkaline phosphatase, *Anal. Methods*, 2022, **15**(1), 79–86, DOI: [10.1039/d2ay01658c](https://doi.org/10.1039/d2ay01658c).
- 83 F. Ma, Q. Zhou, M. Yang, J. Zhang and X. Chen, Microwave-Assisted Synthesis of Sulfur Quantum Dots for Detection of Alkaline Phosphatase Activity, *Nanomaterials*, 2022, **12**(16), 1–10, DOI: [10.3390/nano12162787](https://doi.org/10.3390/nano12162787).
- 84 M. X. Wei, N. Wei, L. F. Pang, X. F. Guo and H. Wang, Determination of dopamine in human serum based on green-emitting fluorescence carbon dots, *Opt. Mater.*, 2021, **118**, 111257, DOI: [10.1016/j.optmat.2021.111257](https://doi.org/10.1016/j.optmat.2021.111257).
- 85 M. Louleb, *et al.*, Detection of Dopamine in Human Fluids Using N-Doped Carbon Dots, *ACS Appl. Nano Mater.*, 2020, **3**(8), 8004–8011, DOI: [10.1021/acsanm.0c01461](https://doi.org/10.1021/acsanm.0c01461).
- 86 S. Hu, D. Qin, S. Meng, Y. Wu, Z. Luo and B. Deng, Cathodic electrochemiluminescence based on resonance energy transfer between sulfur quantum dots and dopamine quinone for the detection of dopamine, *Microchem. J.*, 2022, **181**, 107776, DOI: [10.1016/j.microc.2022.107776](https://doi.org/10.1016/j.microc.2022.107776).
- 87 M. Myśliwiec, K. Zorena, A. Balcerska, J. Myśliwska, P. Lipowski and K. Raczynska, The activity of N-acetyl-beta-d-glucosaminidase and tumor necrosis factor-alpha at early stage of diabetic retinopathy development in type 1 diabetes mellitus children, *Clin. Biochem.*, 2006, **39**(8), 851–856, DOI: [10.1016/j.clinbiochem.2006.03.013](https://doi.org/10.1016/j.clinbiochem.2006.03.013).
- 88 O. P. Mishra, P. Jain, P. Srivastava and R. Prasad, Urinary N-acetyl-beta-D glucosaminidase (NAG) level in idiopathic nephrotic syndrome, *Pediatr. Nephrol.*, 2012, **27**(4), 589–596, DOI: [10.1007/s00467-011-2041-4](https://doi.org/10.1007/s00467-011-2041-4).
- 89 R. B. Kalahasthi, H. R. Rajmohan, B. K. Rajan and K. Kumar M, Urinary N-acetyl-beta-D-glucosaminidase





- and its isoenzymes A & B in workers exposed to cadmium at cadmium plating, *J. Occup. Med. Toxicol.*, 2007, **2**(1), 1–7, DOI: [10.1186/1745-6673-2-5](https://doi.org/10.1186/1745-6673-2-5).
- 90 P. Vibulcharoenkitja, W. Suginta and A. Schulte, Electrochemical N-acetyl- $\beta$ -D-glucosaminidase urinalysis: Toward sensor chip-based diagnostics of kidney malfunction, *Biomolecules*, 2021, **11**(10), 1–12, DOI: [10.3390/biom11101433](https://doi.org/10.3390/biom11101433).
- 91 J. Liu, K. Ning, Y. Fu, Y. Sun and J. Liang, Sulfur quantum dots as a fluorescent sensor for N-acetyl-beta-D-glucosaminidase detection, *Spectrochim. Acta, Part A*, 2023, **294**, 122553, DOI: [10.1016/j.saa.2023.122553](https://doi.org/10.1016/j.saa.2023.122553).
- 92 I. Grabowska, M. Chudy, A. Dybko and Z. Brzozka, Uric acid determination in a miniaturized flow system with dual optical detection, *Sens. Actuators, B*, 2008, **130**(1), 508–513, DOI: [10.1016/j.snb.2007.09.051](https://doi.org/10.1016/j.snb.2007.09.051).
- 93 H. Wang, Q. Lu, Y. Hou, Y. Liu and Y. Zhang, High fluorescence S, N co-doped carbon dots as an ultra-sensitive fluorescent probe for the determination of uric acid, *Talanta*, 2016, **155**, 62–69, DOI: [10.1016/j.talanta.2016.04.020](https://doi.org/10.1016/j.talanta.2016.04.020).
- 94 J. B. He, G. P. Jin, Q. Z. Chen and Y. Wang, A quercetin-modified biosensor for amperometric determination of uric acid in the presence of ascorbic acid, *Anal. Chim. Acta*, 2007, **585**(2), 337–343, DOI: [10.1016/j.aca.2007.01.004](https://doi.org/10.1016/j.aca.2007.01.004).
- 95 G. Yue, *et al.*, Ratiometric fluorescence based on silver clusters and N, Fe doped carbon dots for determination of H<sub>2</sub>O<sub>2</sub> and UA: N, Fe doped carbon dots as mimetic peroxidase, *Sens. Actuators, B*, 2019, **287**, 408–415, DOI: [10.1016/j.snb.2019.02.060](https://doi.org/10.1016/j.snb.2019.02.060).
- 96 C. Zhao, Y. Jiao, F. Hu and Y. Yang, Green synthesis of carbon dots from pork and application as nanosensors for uric acid detection, *Spectrochim. Acta, Part A*, 2018, **190**, 360–367, DOI: [10.1016/j.saa.2017.09.037](https://doi.org/10.1016/j.saa.2017.09.037).
- 97 S. Rong, *et al.*, Novel and facile synthesis of heparin sulfur quantum dots *via* oxygen acceleration for ratiometric sensing of uric acid in human serum, *Sens. Actuators, B*, 2022, **353**, 131146, DOI: [10.1016/j.snb.2021.131146](https://doi.org/10.1016/j.snb.2021.131146).
- 98 B. Kannan, S. Jahanshahi-Anbuhi, R. H. Pelton, Y. Li, C. D. M. Filipe and J. D. Brennan, Printed Paper Sensors for Serum Lactate Dehydrogenase using Pullulan-Based Inks to Immobilize Reagents, *Anal. Chem.*, 2015, **87**(18), 9288–9293, DOI: [10.1021/acs.analchem.5b01923](https://doi.org/10.1021/acs.analchem.5b01923).
- 99 Y. Zhou, M. Qi and M. Yang, Current Status and Future Perspectives of Lactate Dehydrogenase Detection and Medical Implications: A Review, *Biosensors*, 2022, **12**(12), 1–17, DOI: [10.3390/bios12121145](https://doi.org/10.3390/bios12121145).
- 100 G. Rattu, N. Khansili, V. K. Maurya and P. M. Krishna, Lactate detection sensors for food, clinical and biological applications: a review, *Environ. Chem. Lett.*, 2021, **19**(2), 1135–1152, DOI: [10.1007/s10311-020-01106-6](https://doi.org/10.1007/s10311-020-01106-6).
- 101 S. Fan, X. Li, F. Ma, M. Yang, J. Su and X. Chen, Sulfur quantum dot based fluorescence assay for lactate dehydrogenase activity detection, *J. Photochem. Photobiol., A*, 2022, **430**, 113989, DOI: [10.1016/j.jphotochem.2022.113989](https://doi.org/10.1016/j.jphotochem.2022.113989).
- 102 M. Dirak, J. Chan and S. Kolemen, Optical imaging probes for selective detection of butyrylcholinesterase, *J. Mater. Chem. B*, 2024, **12**, 1149–1167, DOI: [10.1039/d3tb02468g](https://doi.org/10.1039/d3tb02468g).
- 103 M. Pohanka, Electrochemical biosensors based on acetylcholinesterase and butyrylcholinesterase. A review, *Int. J. Electrochem. Sci.*, 2016, **11**(9), 7440–7452, DOI: [10.20964/2016.09.16](https://doi.org/10.20964/2016.09.16).
- 104 Y. Miao, N. He and J. J. Zhu, History and new developments of assays for cholinesterase activity and inhibition, *Chem. Rev.*, 2010, **110**(9), 5216–5234, DOI: [10.1021/cr900214c](https://doi.org/10.1021/cr900214c).
- 105 M. Pohanka, Biosensors containing acetylcholinesterase and butyrylcholinesterase as recognition tools for detection of various compounds, *Chem. Pap.*, 2015, **69**(1), 4–16, DOI: [10.2478/s11696-014-0542-x](https://doi.org/10.2478/s11696-014-0542-x).
- 106 Z. Ma, P. Li, M. Jiao, Y. E. Shi, Y. Zhai and Z. Wang, Ratiometric sensing of butyrylcholinesterase activity based on the MnO<sub>2</sub> nanosheet-modulated fluorescence of sulfur quantum dots and o-phenylenediamine, *Microchim. Acta*, 2021, **188**(9), 1–9, DOI: [10.1007/s00604-021-04949-0](https://doi.org/10.1007/s00604-021-04949-0).
- 107 M. Chen, J. Zhang, J. Chang, H. Li, Y. Zhai and Z. Wang, Ultrasensitive detection of butyrylcholinesterase activity based on self-polymerization modulated fluorescence of sulfur quantum dots, *Spectrochim. Acta, Part A*, 2022, **269**, 120756, DOI: [10.1016/j.saa.2021.120756](https://doi.org/10.1016/j.saa.2021.120756).
- 108 N. Amin, A. Afkhami, L. Hosseinzadeh and T. Madrakian, Green and cost-effective synthesis of carbon dots from date kernel and their application as a novel switchable fluorescence probe for sensitive assay of Zoledronic acid drug in human serum and cellular imaging, *Anal. Chim. Acta*, 2018, **1030**, 183–193, DOI: [10.1016/j.aca.2018.05.014](https://doi.org/10.1016/j.aca.2018.05.014).
- 109 M. Caraglia, *et al.*, Stealth liposomes encapsulating zoledronic acid: A new opportunity to treat neuropathic pain, *Mol. Pharmaceutics*, 2013, **10**(3), 1111–1118, DOI: [10.1021/mp3006215](https://doi.org/10.1021/mp3006215).
- 110 J. R. Green, Bisphosphonates: preclinical review, *Oncologist*, 2004, **9**(suppl. 4), 3–13, DOI: [10.1634/theoncologist.9-90004-3](https://doi.org/10.1634/theoncologist.9-90004-3).
- 111 G. Boran, S. Tavakoli, I. Dierking, A. R. Kamali and D. Ege, Synergistic effect of graphene oxide and zoledronic acid for osteoporosis and cancer treatment, *Sci. Rep.*, 2020, **10**(1), 1–12, DOI: [10.1038/s41598-020-64760-4](https://doi.org/10.1038/s41598-020-64760-4).
- 112 S. Faham, R. Ghavami, H. Golmohammadi and G. Khayatian, Spectrophotometric and visual determination of zoledronic acid by using a bacterial cell-derived nanopaper doped with curcumin, *Microchim. Acta*, 2019, **186**(11), 1–18, DOI: [10.1007/s00604-019-3815-9](https://doi.org/10.1007/s00604-019-3815-9).
- 113 J. Tan, *et al.*, Signal-on and selective detection of anti-tumor adjunctive drug zoledronic acid using fluorescent sulfur quantum dots, *Dyes Pigm.*, 2022, **205**, 110520, DOI: [10.1016/j.dyepig.2022.110520](https://doi.org/10.1016/j.dyepig.2022.110520).
- 114 H. Da Silva, J. Pacheco, J. Silva, S. Viswanathan and C. Delerue-Matos, Molecularly imprinted sensor for voltammetric detection of norfloxacin, *Sens. Actuators, B*, 2015, **219**, 301–307, DOI: [10.1016/j.snb.2015.04.125](https://doi.org/10.1016/j.snb.2015.04.125).
- 115 Z. Liu, *et al.*, High-sensitive electrochemical sensor for determination of Norfloxacin and its metabolism using MWCNT-CPE/pRGO-ANSA/Au, *Sens. Actuators, B*, 2018, **257**, 1065–1075, DOI: [10.1016/j.snb.2017.11.052](https://doi.org/10.1016/j.snb.2017.11.052).





- 116 Y. Fu, Y. Xie, H. Shi, G. Zhang, H. Zhang and S. Feng, Molecularly imprinted electrochemical sensor based on metal-covalent organic framework for specifically recognizing norfloxacin from untreated milk, *Food Chem.*, 2023, **429**, 136921, DOI: [10.1016/j.FOODCHEM.2023.136921](https://doi.org/10.1016/j.foodchem.2023.136921).
- 117 P. Koutsogiannis, E. Thomou, H. Stamatis, D. Gournis and P. Rudolf, Advances in fluorescent carbon dots for biomedical applications, *Adv. Phys. X*, 2020, **5**(1), 1–37, DOI: [10.1080/23746149.2020.1758592](https://doi.org/10.1080/23746149.2020.1758592).
- 118 H. Zhang, J. You, J. Wang, X. Dong, R. Guan and D. Cao, Highly luminescent carbon dots as temperature sensors and 'off-on' sensing of Hg<sup>2+</sup> and biothiols, *Dyes Pigm.*, 2020, **173**, 107950, DOI: [10.1016/j.dyepig.2019.107950](https://doi.org/10.1016/j.dyepig.2019.107950).
- 119 Y. Jiang, *et al.*, Preparation of dual-emission polyurethane/carbon dots thermoresponsive composite films for colorimetric temperature sensing, *Carbon*, 2020, **163**, 26–33, DOI: [10.1016/j.carbon.2020.03.013](https://doi.org/10.1016/j.carbon.2020.03.013).
- 120 R. B. González-González, A. Sharma, R. Parra-Saldívar, R. A. Ramirez-Mendoza, M. Bilal and H. M. N. Iqbal, Decontamination of emerging pharmaceutical pollutants using carbon dots as robust materials, *J. Hazard. Mater.*, 2022, **423**, 1–19, DOI: [10.1016/j.jhazmat.2021.127145](https://doi.org/10.1016/j.jhazmat.2021.127145).
- 121 S. Menon and K. G. Kumar, Simultaneous Voltammetric Determination of Acetaminophen and Its Fatal Counterpart Nimesulide by Gold Nano/L-Cysteine Modified Gold Electrode, *J. Electrochem. Soc.*, 2017, **164**(9), B482–B487, DOI: [10.1149/2.0181712jes](https://doi.org/10.1149/2.0181712jes).
- 122 J. Song, X. Liang, Q. Ma, J. An and F. Feng, Fluorescent boron and nitrogen co-doped carbon dots with high quantum yield for the detection of nimesulide and fluorescence staining, *Spectrochim. Acta, Part A*, 2019, **216**, 296–302, DOI: [10.1016/j.saa.2019.03.074](https://doi.org/10.1016/j.saa.2019.03.074).
- 123 J. Song, *et al.*, A simple preparation method of carbon dots by weak power bathroom lamp irradiation and their application for nimesulide detection and bioimaging, *RSC Adv.*, 2018, **8**(63), 36090–36095, DOI: [10.1039/c8ra06313c](https://doi.org/10.1039/c8ra06313c).
- 124 Q. Ma, *et al.*, Small molecule L-cysteine assisted synthesis of green fluorescent sulfur quantum dots for nimesulide sensing and bioimaging, *Microchem. J.*, 2023, **190**, 108734, DOI: [10.1016/j.microc.2023.108734](https://doi.org/10.1016/j.microc.2023.108734).
- 125 R. A. Cherny, *et al.*, Treatment with a copper-zinc chelator markedly and rapidly inhibits  $\beta$ -amyloid accumulation in Alzheimer's disease transgenic mice, *Neuron*, 2001, **30**(3), 665–676, DOI: [10.1016/S0896-6273\(01\)00317-8](https://doi.org/10.1016/S0896-6273(01)00317-8).
- 126 S. Maheshwaran, *et al.*, Electrocatalytic evaluation of graphene oxide warped tetragonal t-lanthanum vanadate (GO@LaVO<sub>4</sub>) nanocomposites for the voltammetric detection of antifungal and antiprotozoal drug (clioquinol), *Microchim. Acta*, 2021, **188**(3), 1–9, DOI: [10.1007/s00604-021-04758-5](https://doi.org/10.1007/s00604-021-04758-5).
- 127 R. K. Devi, *et al.*, Oxygen-terminated vanadium carbide with graphitic carbon nitride nanosheets modified electrode: A robust electrochemical platform for the sensitive detection of antibiotic drug clioquinol, *Process Saf. Environ. Prot.*, 2023, **172**, 986–997, DOI: [10.1016/j.PSEP.2023.02.049](https://doi.org/10.1016/j.psep.2023.02.049).
- 128 Q. Tan, X. An, S. Pan, S. Zhen, Y. Hu and X. Hu, One-pot hydrothermal method synthesis carbon dots as a fluorescent sensor for the sensitive and selective detection of clioquinol, *Opt. Mater.*, 2022, **123**, 111830, DOI: [10.1016/J.OPTMAT.2021.111830](https://doi.org/10.1016/j.optmat.2021.111830).
- 129 J. Zhao and Z. Fan, Using zinc ion-enhanced fluorescence of sulfur quantum dots to improve the detection of the zinc(II)-binding antifungal drug clioquinol, *Microchim. Acta*, 2020, **187**(3), 1–8.
- 130 Z. Mu, J. Hua, S. Feng and Y. Yang, A ratiometric fluorescence and light scattering sensing platform based on Cu-doped carbon dots for tryptophan and Fe(III), *Spectrochim. Acta, Part A*, 2019, **219**, 248–256, DOI: [10.1016/j.saa.2019.04.065](https://doi.org/10.1016/j.saa.2019.04.065).
- 131 W. Li, *et al.*, Pyridine functionalized carbon dots for specific detection of tryptophan in human serum samples and living cells, *Microchem. J.*, 2020, **154**, 104579, DOI: [10.1016/j.microc.2019.104579](https://doi.org/10.1016/j.microc.2019.104579).
- 132 W. Jiang, R. He, H. Lv, X. He, L. Wang and Y. Wei, Chiral Sensing of Tryptophan Enantiomers Based on the Enzyme Mimics of  $\beta$ -Cyclodextrin-Modified Sulfur Quantum Dots, *ACS Sens.*, 2023, **8**(11), 4264–4271, DOI: [10.1021/acssensors.3c01616](https://doi.org/10.1021/acssensors.3c01616).

